

Spectral Decomposition Representation for Reinforcement Learning

Tongzheng Ren^{1, 2, *} Tianjun Zhang^{3, *} Lisa Lee¹ Joseph E. Gonzalez³
Dale Schuurmans^{1, 4} Bo Dai¹

¹ Google Research, Brain Team ² UT Austin ³ UC Berkeley ⁴ University of Alberta

Abstract

Representation learning often plays a critical role in reinforcement learning by managing the curse of dimensionality. A representative class of algorithms exploits a spectral decomposition of the stochastic transition dynamics to construct representations that enjoy strong theoretical properties in an idealized setting. However, current spectral methods suffer from limited applicability because they are constructed for state-only aggregation and derived from a policy-dependent transition kernel, without considering the issue of exploration. To address these issues, we propose an alternative spectral method, *Spectral Decomposition Representation* (SPEDER), that extracts a state-action abstraction from the dynamics without inducing spurious dependence on the data collection policy, while also balancing the exploration-versus-exploitation trade-off during learning. A theoretical analysis establishes the sample efficiency of the proposed algorithm in both the online and offline settings. In addition, an experimental investigation demonstrates superior performance over current state-of-the-art algorithms across several benchmarks.

1 Introduction

Reinforcement learning (RL) seeks to learn optimal sequential decisions by interacting with an unknown environment, which is usually modeled by a Markov decision process (MDP). For MDPs with finite states and actions, RL can be solved in a sample and computationally efficient way. However, the cost of RL algorithms quickly becomes expensive with larger or infinite state spaces.

Representation learning is a major tool to combat the curse of dimensionality, and has led to several empirical successes in deep RL [Mnih et al., 2015, Levine et al., 2016, Silver et al., 2017, Bellemare et al., 2020], where policies and value functions are represented as deep neural networks and trained end-to-end. However, an inappropriate representation may induce redundant solutions to the empirical Bellman error, whose generalization error is large, as shown in [Xiao et al., 2021]. Therefore, representation learning becomes even more important in deep RL. In prior work, many methods have been proposed to ensure different properties of the representation, such as reconstruction [Watter et al., 2015], bi-simulation [Gelada et al., 2019], and invariance preservation [Zhang et al., 2020].

Among these methods, a family of representation learning algorithms has focused on constructing features by exploiting the spectral decomposition of different transition operators, including successor features [Dayan, 1993, Machado et al., 2018], proto-value functions [Mahadevan and Maggioni, 2007, Wu et al., 2018], spectral state aggregation [Duan et al., 2019, Zhang and Wang, 2019], and Krylov bases [Petrik, 2007, Parr et al., 2008]. Although these algorithms look different at first glance, they all essentially factorize some variant of the transition kernel. The most attractive property of such representations is that the value function can be *linearly* represented, thereby reducing the complexity of subsequent planning. Moreover, spectral representations are compatible with deep neural networks [Barreto et al., 2017], making their usage simple for optimal policy learning [Kulkarni et al., 2016b] in deep RL.

*Equal Contribution

However, despite their elegance and desirable properties, existing spectral representation algorithms have several drawbacks. One limitation is that current spectral representations generate *state-only* features, which can be spuriously induced by the behavior policy and fail to generalize across different policies. Moreover, most existing algorithms omit the intimate coupling between representation learning and exploration, and instead learn the representation from a static dataset. This is problematic since efficient exploration depends on having a good representation, and the learning of the representation requires comprehensively-covered experience from exploration. These aforementioned drawbacks result in suboptimal features and limited empirical performance.

In this paper, we address these important but largely ignored issues, and provide a novel spectral representation learning method, which generates a policy-independent features that provably manage the delicate balance between exploration and exploitation. In summary:

- We unify existing representation learning methods in a spectral decomposition view, and identify the cause of spurious dependencies in state-only spectral features (Section 2.2).
- We develop a novel objective, *Spectral Decomposition Representation (SPEDER)*, that factorizes the state-action transition kernel to eliminate policy-induced dependencies (Section 3).
- We provide algorithms that implement the principles of optimism and pessimism in the face of uncertainty using the SPEDER feature for online and offline RL (Section 3.1), and equip behavior cloning with SPEDER for imitation learning (Section 3.2).
- We analyze the sample complexity of SPEDER in both the online and offline settings, to justify the achieved balance between exploration versus exploitation (Section 4).
- We demonstrate that SPEDER outperforms state-of-the-art model-based and model-free RL algorithms on several benchmarks (Section 6).

2 Preliminaries

In this section, we briefly introduce Markov Decision Processes (MDPs) with a low-rank structure, and reveal the spectral decomposition view of several representation learning algorithms, which motivates our new spectral representation learning algorithm.

2.1 Low-Rank Markov Decision Processes

Markov Decision Processes (MDPs) are a standard sequential decision-making model for RL, and can be described as a tuple $\mathcal{M} = (\mathcal{S}, \mathcal{A}, r, P, \rho, \gamma)$, where \mathcal{S} is the state space, \mathcal{A} is the action space, $r : \mathcal{S} \times \mathcal{A} \rightarrow [0, 1]$ is the reward function, $P : \mathcal{S} \times \mathcal{A} \rightarrow \Delta(\mathcal{S})$ is the transition operator, $\rho \in \Delta(\mathcal{S})$ is the initial distribution and $\gamma \in (0, 1)$ is the discount factor. The goal of RL is to find a policy $\pi : \mathcal{S} \rightarrow \Delta(\mathcal{A})$ that maximizes the cumulative discounted reward $V_{P,r}^\pi := \mathbb{E}_{s_0 \sim \rho, \pi} [\sum_{i=0}^{\infty} \gamma^i r(s_i, a_i) | s_0]$, by interacting with the MDP. The value function is defined as $V_{P,r}^\pi(s) = \mathbb{E}_\pi [\sum_{i=0}^{\infty} \gamma^i r(s_i, a_i) | s_0 = s]$, and the action-value function is $Q_{P,r}^\pi(s, a) = \mathbb{E}_\pi [\sum_{i=0}^{\infty} \gamma^i r(s_i, a_i) | s_0 = s, a_0 = a]$. These definitions imply the following recursive relationships:

$$V_{P,r}^\pi(s) = \mathbb{E}_\pi [Q_{P,r}^\pi(s, a)], \quad Q_{P,r}^\pi(s, a) = r(s, a) + \gamma \mathbb{E}_P [V_{P,r}^\pi(s')].$$

We additionally define the state visitation distribution induced by a policy π as $d_P^\pi(s) = (1 - \gamma) \mathbb{E}_{s_0 \sim \rho, \pi} [\sum_{t=0}^{\infty} \gamma^t \mathbf{1}(s_t = s) | s_0]$, where $\mathbf{1}(\cdot)$ is the indicator function. When $|\mathcal{S}|$ and $|\mathcal{A}|$ are finite, there exist sample-efficient algorithms that find the optimal policy by maintaining an estimate of P or $Q_{P,r}^\pi$ [Azar et al., 2017, Jin et al., 2018]. However, such methods cannot be scaled up when $|\mathcal{S}|$ and $|\mathcal{A}|$ are extremely large or infinite. In such cases, function approximation is needed to exploit the structure of the MDP while avoiding explicit dependence on $|\mathcal{S}|$ and $|\mathcal{A}|$. The low rank MDP is one of the most prominent structures that allows for simple yet effective function approximation in MDPs, which is based on the following spectral structural assumption on P and r :

Assumption 1 (Low Rank MDP, [Jin et al., 2020, Agarwal et al., 2020]). *An MDP \mathcal{M} is a low rank MDP if there exists a low rank spectral decomposition of the transition kernel $P(s'|s, a)$, such that*

$$P(s'|s, a) = \langle \phi(s, a), \mu(s') \rangle, \quad r(s, a) = \langle \phi(s, a), \theta_r \rangle, \quad (1)$$

with two spectral maps $\phi : \mathcal{S} \times \mathcal{A} \rightarrow \mathbb{R}^d$ and $\mu : \mathcal{S} \rightarrow \mathbb{R}^d$, and a vector $\theta_r \in \mathbb{R}^d$. The ϕ and μ also satisfy the following normalization conditions:

$$\forall (s, a), \|\phi(s, a)\|_2 \leq 1, \|\theta_r\|_2 \leq \sqrt{d}, \forall g : \mathcal{S} \rightarrow \mathbb{R}, \|g\|_{L_\infty} \leq 1, \|\int_{\mathcal{S}} \mu(s') g(s') ds'\|_2 \leq \sqrt{d}. \quad (2)$$

The low rank MDP allows for a linear representation of $Q_{P,r}^\pi$ for any *arbitrary* policy π , since

$$Q_{P,r}^\pi(s, a) = r(s, a) + \gamma \int V_{P,r}^\pi(s') P(s'|s, a) ds' = \langle \phi(s, a), \theta_r + \gamma \int V_{P,r}^\pi(s') \mu(s') ds' \rangle.$$

Hence, we can provably perform computationally-efficient planning and sample-efficient exploration in Low-rank MDP, as shown in [Jin et al., 2020]. However, $\phi(s, a)$ is generally not given to the

reinforcement learning algorithm, and must be learned via representation learning in order to leverage the structure of low rank MDPs.

2.2 Spectral Framework for Representation Learning

Representation learning based on a spectral decomposition of the transition dynamics was investigated as early as [Dayan \[1993\]](#), although the explicit study began with [Mahadevan and Maggioni \[2007\]](#), which constructed features via eigenfunctions from Laplacians of the transitions. This inspired a series of subsequent work on spectral decomposition representations, including the Krylov basis [[Petrik, 2007](#), [Parr et al., 2008](#)], continuous Laplacian [Wu et al. \[2018\]](#), and spectral state aggregation [[Duan et al., 2019](#), [Zhang and Wang, 2019](#)]. We summarize these algorithms in Table 1 to reveal their common drawbacks, which motivates the development of a new algorithm. A similar summary has been provided in [[Ghosh and Bellemare, 2020](#)].

These previous spectral representation methods construct features based on the spectral space of the state transition probability $P^\pi(s'|s) = \int P(s'|s, a)\pi(a|s)da$, induced by some policy π . Compared with the policy-independent feature for Low-rank MDP, such a transition operator introduces inter-state dependency based on a specific policy π , which injects an inductive bias into the state-only spectral representation, resulting in features that might not be generalizable to other policies. To make the state-feature generalizable, some work resort to the linear action model [e.g. [Yao and Szepesvári, 2012](#), [Gehring et al., 2018](#)] where the action information is stored in the linear weight.

However, these work requires known state-feature, and it is not clear on how to combine the linear action model with the spectral feature framework. Moreover, these existing spectral representation methods completely ignore the problem of exploration, which affects dataset composition for representation learning, and is conversely affected by the learned representation during the data collection procedure. These drawbacks have limited the performance of spectral representations.

Table 1: A unified spectral decomposition view of existing related representations. Here, r denotes the reward function, Λ denotes some diagonal reweighting operator, and $P^\pi(s'|s) = \int P(s'|s, a)\pi(a|s)da$. We purposely omit the decomposition algorithms of each representation to reveal the unified view.

Representation	Decomposed Dynamics
Successor Feature	$\text{svd}((I - \gamma P^\pi)^{-1})$
Proto-Value Function	$\text{eig}(\Lambda P^\pi + (P^\pi)^\top \Lambda)$
Krylov Basis	$\{(P^\pi)^i r\}_{i=1}^k$
Spectral State-Aggregation	$\text{svd}(P^\pi)$

3 Spectral Decomposition Representation Learning

To address these issues, we provide a novel spectral decomposition optimization surrogate, which we refer to as Spectral Decomposition Representation (SPEDER). SPEDER is compatible with stochastic gradient updates, and is therefore naturally applicable to general practical settings. We will show that SPEDER can be easily combined with the principle of optimism in the face of uncertainty to obtain sample efficient online exploration, and can also be leveraged to perform latent behavioral cloning.

As discussed in Section 2, the fundamental cause of the spurious dependence in state-only spectral features arises from the state transition operator $P^\pi(s'|s)$, which introduces inter-state dependence induced by a specific behavior policy π . To resolve this issue, we extract the spectral feature from $P(s'|s, a)$ alone, which is invariant to the policy, thereby resulting in a more stable spectral representation. Assume we are given a set of observations $\{(s_i, a_i, s'_i)\}_{i=1}^n$ sampled from $\rho_0(s, a) \times P(s'|s, a)$, and want to learn spectral features $\phi(s, a)$ and $\mu(s')$, with $\phi \in \Phi$, $\mu \in \Psi$ produced by function approximators like deep neural nets, such that:

$$P(s'|s, a) \approx \phi(s, a)^\top \mu(s'). \quad (3)$$

As discussed in Section 2.1, such a representation allows for a simple linear parameterization of Q for any policy π , making the planning step efficient. Note that (3) can be viewed as a density estimation problem, and we can apply maximum likelihood estimation (MLE) to estimate ϕ and μ :

$$(\hat{\phi}, \hat{\mu}) = \arg \max_{\phi \in \Phi, \mu \in \Psi} \frac{1}{n} \sum_{i=1}^n \log \phi(s_i, a_i)^\top \mu(s'_i) - \log Z(s, a), \quad (4)$$

where $Z(s, a) = \int_S \phi(s, a)^\top \mu(s') ds'$. In fact, [[Agarwal et al., 2020](#), [Uehara et al., 2021](#)] provide rigorous theoretical guarantees when a computation oracle for solving (4) is provided. However, such a computation is highly nontrivial. Note that the MLE (4) is invariant to the scale of ϕ and μ ; that is, if (ϕ, μ) is a solution of (4), then $(c_1\phi, c_2\mu)$ is also a solution of (4) for any $c_1, c_2 > 0$. Hence, we generally do not have $Z(s, a) = 1$ for any (s, a) , and we can only use $P(s'|s, a) = \left(\frac{\phi(s, a)}{Z(s, a)}\right)^\top \mu(s')$.

Therefore, we need to use $\tilde{\phi}(s, a) := \frac{\phi(s, a)}{Z(s, a)}$ to linearly represent the Q -function, which incurs an extra estimation requirement for $Z(s, a)$.

To eliminate the scaling issue in the optimal solution to (4), we draw inspiration from the spectral method for conditional density estimation [Grünwälder et al., 2012] and consider the population objective:

$$\mathbb{E}_{(s,a) \sim \rho_0} \|P(\cdot|s, a) - \phi(s, a)^\top \mu(\cdot)\|_2^2, \quad (5)$$

where the L_2 norm of the function $f(s')$ is defined as $\|f(s')\|_2^2 := \int_{\mathcal{S}} f(s')^2 ds'$. This objective (5) has a unique global minimum, $\phi(s, a)^\top \mu(s') = P(s'|s, a)$, thus it can be used as an alternative representation learning objective.

However, the objective (5) has several issues, one being that it has an explicit dependence on P , but we can only access samples from P . To resolve this issue, we note that

$$\begin{aligned} L(\phi, \mu) &:= \mathbb{E}_{(s,a) \sim \rho_0} \|P(\cdot|s, a) - \phi(s, a)^\top \mu(\cdot)\|_2^2 \\ &= C - 2\mathbb{E}_{(s,a) \sim \rho_0, s' \sim P(s'|s, a)} [\phi(s, a)^\top \mu(s')] + \mathbb{E}_{(s,a) \sim \rho_0} \left[\int_{\mathcal{S}} (\phi(s, a)^\top \mu(s'))^2 ds' \right], \end{aligned} \quad (6)$$

where $C = \mathbb{E}_{s,a \sim \rho_0} \left[\int (P(s'|s, a))^2 \right]$ is a problem-dependent constant. With this expression (6), we can use the following Monte Carlo estimate to approximate the population objective:

$$\hat{L}(\phi, \mu) := -\frac{2}{n} \sum_{i=1}^n \phi(s_i, a_i) \mu(s'_i) + \frac{1}{n} \sum_{i=1}^n \left[\int_{\mathcal{S}} (\phi(s_i, a_i)^\top \mu(s'))^2 ds' \right]. \quad (7)$$

This approach only requires the samples from P , but at a cost of estimating the term $\int_{\mathcal{S}} (\phi(s, a)^\top \mu(s'))^2 ds'$. Generally, such terms cannot be computed exactly if we do not have specific structure on ϕ and μ . Hence, we turn to an approximation method by choosing $\mu(s') = p(s')\mu'(s')$, where $p(s')$ is a probability measure supported on the state space \mathcal{S} . Then we rewrite such term as

$$\mathbb{E}_{(s,a) \sim \rho_0} \left[\int_{\mathcal{S}} (\phi(s, a)^\top \mu(s'))^2 ds' \right] = \text{Trace} \left(\mathbb{E}_{(s,a) \sim \rho_0} [\phi(s, a)\phi(s, a)^\top] \mathbb{E}_p [p(s')\mu'(s')\mu'(s')^\top] \right).$$

Now, $\mathbb{E}_{(s,a) \sim \rho_0} [\phi(s, a)\phi(s, a)^\top]$ and $\mathbb{E}_p [p(s')\mu'(s')\mu'(s')^\top]$ can both be approximated by Monte Carlo estimates. However, both terms are $d \times d$ matrices, which require large samples to approximate accurately. Motivated by the orthogonality of the spectral representation, we can constrain ϕ to satisfy $\mathbb{E}_{s,a} [\phi(s, a)\phi(s, a)^\top] = I_d/d$ where $1/d$ is the normalizing factor due to the assumption that $\|\phi(s, a)\| \leq 1$. With this condition, we can write

$$\text{Trace} \left(\mathbb{E}_{(s,a) \sim \rho_0} [\phi(s, a)\phi(s, a)^\top] \mathbb{E}_p [p(s')\mu'(s')\mu'(s')^\top] \right) = \mathbb{E}_p [p(s')\mu'(s')^\top \mu'(s')] / d.$$

Hence, the eventual representation learning objective can be written as:

$$\begin{aligned} \min_{\phi, \mu'} & -\mathbb{E}_{(s,a,s') \sim \rho_0 \times P} [\phi(s, a)^\top \mu'(s') p(s')] + (\mathbb{E}_{p(s')} [p(s')\mu'(s')^\top \mu'(s')]) / (2d) \\ \text{s.t. } & \mathbb{E}_{(s,a) \sim \rho_0} [\phi(s, a)\phi(s, a)^\top] = I_d/d, \end{aligned} \quad (8)$$

As (8) can be approximated with the samples, it can be solved via stochastic gradient updates, where the constraint is handled via the penalty method as Wu et al. [2018]. The algorithm is in stark contrast to existing methods for spectral features by explicit eigendecomposition of transition matrices in [Mahadevan and Maggioni, 2007, Machado et al., 2017, 2018].

Equivalent model-free spectral representation learning: Instead of considering the L_2 model error minimization (6), the state-action spectral representation can also be derived equivalently from a model-free SVD perspective. Specifically, the SVD of transition operator can be formulated as

$$\begin{aligned} & \max_{\mathbb{E}[\phi\phi^\top] = I_d} \left\| \langle P(s'|s, a), \phi(s, a)^\top \rangle_{\rho_0} \right\|^2 \\ &= \max_{\mathbb{E}[\phi\phi^\top] = I_d/d} \max_{\mu} 2\text{Trace} \left(\mathbb{E}_{\rho_0} \left[\int \mu(s') P(s'|s, a) \phi(s, a)^\top ds' \right] \right) - 1/d \int \mu(s')^\top \mu(s') ds' \\ &= \max_{\phi, \mu'} 2\mathbb{E}_{\rho_0 \times P} [\phi(s, a)^\top \mu'(s') p(s')] - \mathbb{E}_p [p(s')\mu'(s')^\top \mu'(s')] / d, \quad \text{s.t. } \mathbb{E}[\phi\phi^\top] = I_d/d, \end{aligned}$$

which is equivalent to (8), showing an interesting connection between model-based and model-free representation learning through duality. The second equality comes from the Fenchel duality of $\|\cdot\|^2$ with up-scaling of μ by \sqrt{d} , and the third equality comes from $\mu(s') = p(s')\mu'(s')$.

Algorithm 1 Online Exploration with SPEDER

- 1: **Input:** Regularizer λ_n , parameter α_n , Model class $\mathcal{F} = \{(\phi, \mu) : \phi \in \Phi, \mu \in \Psi, \}$, Iteration N
 - 2: Initialize $\pi_0(\cdot | s)$ to be uniform; set $\mathcal{D}_0 = \emptyset, \mathcal{D}'_0 = \emptyset$
 - 3: **for** episode $n = 1, \dots, N$ **do**
 - 4: Collect the transition $(s, a, s', a', \tilde{s})$ where $s \sim d_{P^*}^{\pi_{n-1}}, a \sim \mathcal{U}(\mathcal{A}), s' \sim P^*(\cdot | s, a), a' \sim \mathcal{U}(\mathcal{A}), \tilde{s} \sim P^*(\cdot | s', a')$, where $\mathcal{U}(\mathcal{A})$ denotes the uniform distribution on \mathcal{A} .
 - 5: $\mathcal{D}_n = \mathcal{D}_{n-1} \cup \{s, a, s'\}, \mathcal{D}'_n = \mathcal{D}'_{n-1} \cup \{s', a', \tilde{s}\}.$
 - 6: Learn representation $\hat{\phi}(s, a)$ with $\mathcal{D}_n \cup \mathcal{D}'_n$ via (8).
 - 7: Update the empirical covariance matrix

$$\hat{\Sigma}_n = \sum_{s,a \in \mathcal{D}_n} \hat{\phi}_n(s, a) \hat{\phi}_n(s, a)^\top + \lambda_n I$$
 - 8: Set the exploration bonus $\hat{b}_n(s, a) = \alpha_n \sqrt{\hat{\phi}_n(s, a)^\top \hat{\Sigma}_n^{-1} \hat{\phi}_n(s, a)}$
 - 9: Update policy $\pi_n = \arg \max_{\pi} V_{\hat{P}_n, r + \hat{b}_n}^\pi$
 - 10: **end for**
 - 11: **Return** π_1, \dots, π_N
-

3.1 Online Exploration and Offline Policy Optimization with SPEDER

Unlike existing spectral representation learning algorithms, which focus on the offline setting, we can use SPEDER to perform sample efficient online exploration. In Algorithm 1, we show how to use the representation obtained from the solution to (8) to perform sample efficient online exploration under the principle of optimism in the face of uncertainty. Central to the algorithm is the newly proposed representation learning procedure (Line 6 in Algorithm 1), which learns the representation $\hat{\phi}(s, a)$ and the model $\hat{P}(s' | s, a) = \hat{\phi}(s, a)^\top \hat{\mu}(s, a)$ with adaptively collected exploratory data. After recovering the representation, we use the standard elliptical potential [Jin et al., 2020, Uehara et al., 2021] as the bonus (Line 8 in Algorithm 1) to enforce exploration. We then plan using the learned model \hat{P}_n with the reward bonus \hat{b}_n to obtain a new policy that is used to collect additional exploratory data.

SPEDER can also be combined with the pessimism principle to perform sample efficient offline policy optimization. Unlike the online setting where we enforce exploration by adding a bonus to the reward, we now *subtract* the elliptical potential from the reward to avoid risky behavior. For completeness, we include the algorithm for offline policy optimization in Appendix B.

On the requirements of \hat{P}_n . As we need to plan with the learned model \hat{P}_n , we generally require \hat{P}_n to be a valid transition kernel, but the representation learning objective (8) does not explicitly enforce this. Therefore in our implementations, we just use the data from the replay buffer collected during the past executions to perform planning. We can also enforce that \hat{P}_n is a valid probability by optimizing an additional regularization term:

$$\mathbb{E}_{(s,a)} \left[\left(\log \int_{\mathcal{S}} \phi(s, a)^\top \mu'(s') p(s') ds' \right)^2 \right], \quad (9)$$

which can be approximated with samples from $p(s')$.

Practical Implementation We parameterize $\phi(s, a)$ and $\mu(s')$ as separate MLP networks, and train them by optimizing the objective (8). Instead of using the linear Q on top of $\phi(s, a)$ suggested by the low-rank MDP, we parameterize the critic network as a two-layer MLP network on top of the learned representation $\phi(s, a)$ to support the nonlinear exploration bonus and entropy regularization. Unlike other representation learning methods in RL, we do not backpropagate the gradient from TD-learning to the representation network $\phi(s, a)$. To train the policy, we use the Soft Actor-Critic (SAC) algorithm [Haarnoja et al., 2018], and alternate between policy optimization and critic training.

3.2 Spectral Representation for Latent Behavioral Cloning

We additionally experiment with using the learned representations $\phi(s, a)$ for downstream imitation learning, which is a framework for learning a behavior policy that mimics a given set of expert demonstrations. We assume access to a fixed set of expert transitions $\mathcal{D}^{\pi^*} = \{(s_t, a_t, s_{t+1}) : s_t \sim d_P^{\pi^*}, a_t \sim \pi^E(s_t), s_{t+1} \sim P(s' | s_t, a_t)\}$. We additionally assume access to a suboptimal dataset of offline transitions $\mathcal{D}^{\text{off}} = \{(s, a, s')\}$ from the same MDP, which is collected by a non-expert policy (e.g., an exploratory policy), whose state distribution $d^{\text{off}}(s)$ may be unknown. We assume that \mathcal{D}^{off} sufficiently covers the expert distribution, i.e., if $d^{\pi^*}(s) > 0$, then $d^{\text{off}}(s) > 0$ for all $s \in \mathcal{S}$. In practice, while expert demonstrations can be expensive to acquire, non-expert data of interactions in

the same environment can be more accessible to collect at scale, and provide additional information about the transition dynamics of the environment.

Latent behavioral cloning [Yang et al., 2021, Yang and Nachum, 2021] consists of a pre-training phase that learns a representation $\phi : \mathcal{S} \times \mathcal{A} \rightarrow Z$ and a policy decoder $\pi_\alpha : \mathcal{S} \times Z \rightarrow \Delta(\mathcal{A})$ on the basis of the suboptimal dataset \mathcal{D}^{off} . Then, a downstream imitation phase learns a latent policy $\pi_Z : \mathcal{S} \rightarrow \Delta(Z)$ using the expert dataset \mathcal{D}^{π^*} . With SPEDER, we perform the latent behavior cloning as follows:

1. **Pretraining Phase:** We pre-train $\phi(s, a)$ and $\mu(s')$ on \mathcal{D}^{off} by minimizing the objective (8). Additionally, we train a policy decoder $\pi_\alpha(a \mid s, \phi(s, a))$ that maps latent action representations to actions in the original action space, by minimizing the action decoding error:

$$\mathbb{E}_{s \sim d_P^{\text{off}}} [-\log \pi_\alpha(a \mid s, \phi(s, a))]$$

2. **Downstream Imitation Phase:** We train a latent policy $\pi_Z : \mathcal{S} \rightarrow \Delta(Z)$ by minimizing the latent behavioral cloning error:

$$\mathbb{E}_{(s,a) \sim d_P^{\pi^*}} [-\log \pi_Z(\phi(s, a) \mid s)]$$

At inference time, given the current state $s \in \mathcal{S}$, we sample a latent action representation $z \sim \pi_Z(s)$, then decode the action $a \sim \pi_\alpha(a \mid s, z)$.

4 Theoretical Analysis

In this section, we establish generalization properties of the proposed representation learning algorithm, and provide sample complexity and error bounds when the proposed representation learning algorithm is applied to online exploration and offline policy optimization.

4.1 Non-asymptotic Generalization Bound

We first state a performance guarantee on the representation learned with the proposed objective.

Theorem 1. Assume the size of candidate model class $|\mathcal{F}| < \infty$, $P \in \mathcal{F}$, and for any $\tilde{P} \in \mathcal{F}$, $\tilde{P}(s' \mid s, a) \leq C$ for all (s, a, s') . Given the dataset $\mathcal{D} := \{(s_i, a_i, s'_i)\}_{i=1}^n$ where $(s_i, a_i) \sim \rho_0$, $s'_i \sim P(\cdot \mid s_i, a_i)$, the estimator \hat{P} obtained by (7) satisfies the following inequality with probability at least $1 - \delta$:

$$\mathbb{E}_{(s,a) \sim \rho_0} \|P(\cdot \mid s, a) - \hat{P}(\cdot \mid s, a)\|_2^2 \leq \frac{C' \log |\mathcal{F}| / \delta}{n}, \quad (10)$$

where C' is a constant that only depends on C , which we will omit in the following analysis.

Note that the i.i.d data assumption can be relaxed to an assumption that the data generating process is a martingale process. This is essential for proving the sample complexity of online exploration, as the data are collected in an adaptive manner. The proofs are deferred to Appendix C.1.

4.2 Sample Complexities of Online Exploration and Offline Policy Optimization

Next, we establish sample complexities for the online exploration and offline policy optimization problems. We still assume $P \in \mathcal{F}$. As the generalization bound (10) only guarantees the expected L_2 distance, we need to make the following additional assumptions on the representation and reward:

Assumption 2 (Representation Normalization). $\forall \phi \in \Phi$, we have $\int_{\mathcal{S}} (\int_{\mathcal{A}} \|\phi(s, a)\|_2 da)^2 ds \leq d$.

Assumption 3 (Reward Normalization). $\int_{\mathcal{S}} (\int_{\mathcal{A}} r(s, a) da)^2 ds \leq d$, where r is the reward function.

A simple example that satisfies both Assumption 2 and 3 is a tabular MDP with features $\phi(s, a)$ forming the canonical basis in $\mathbb{R}^{|\mathcal{S}||\mathcal{A}|}$. In this case, we have $d = |\mathcal{S}||\mathcal{A}|$, hence Assumption 2 naturally holds. Furthermore, since $r(s, a) \in [0, 1]$, it is also straightforward to verify that Assumption 3 holds for a tabular MDP. Such assumption can also be satisfied for continue state space with the volume of the state space $\mu(\mathcal{S}) \leq \frac{d}{|\mathcal{A}|}$. Since we need to plan on \hat{P} , we also assume that \hat{P} is a valid transition kernel. With Assumptions 2 and 3 in hand, we are now ready to provide the sample complexities of online exploration and offline policy optimization. The proofs are deferred to Appendix C.2 and C.3.

Theorem 2 (PAC Guarantee for Online Exploration). Assume $|\mathcal{A}| < \infty$. After interacting with the environment for $N = \tilde{\Theta} \left(\frac{d^4 |\mathcal{A}|^2}{(1-\gamma)^6 \epsilon^2} \right)$ episodes where $\tilde{\Theta}$ omits the log-factors, we can obtain a policy π such that

$$V_{P,r}^{\pi^*} - V_{P,r}^{\pi} \leq \epsilon$$

with high probability, where π^* is the optimal policy. Furthermore, note that, we can obtain a sample from the state visitation distribution d_P^{π} via terminating with probability $1 - \gamma$ for each step. Hence, for each episode, we can terminate within $\tilde{\Theta}(1/(1 - \gamma))$ steps with high probability.

Theorem 3 (PAC Guarantee for Offline Policy Optimization). *Let $\omega = \min_{s,a} \frac{1}{\pi_b(a|s)}$ where π_b is the behavior policy. With probability $1 - \delta$, for all baseline policies π including history-dependent non-Markovian policies, we have that*

$$V_{P,r}^\pi - V_{\hat{P},r}^\pi \lesssim \sqrt{\frac{\omega^2 d^4 C_\pi^* \log(|\mathcal{F}|/\delta)}{(1-\gamma)^6}},$$

where C_π^* is the relative conditional number under ϕ^* which measures the quality of the offline data:

$$C_\pi^* := \sup_{x \in \mathbb{R}} \frac{x^\top \mathbb{E}_{(s,a) \sim d_P} [\phi^*(s,a) \phi^*(s,a)^\top] x}{x^\top \mathbb{E}_{(s,a) \sim \rho_b} [\phi^*(s,a) \phi^*(s,a)^\top] x},$$

5 Related Work

Aside from the family of spectral decomposition representation methods reviewed in Section 2, there have been many attempts to provide **algorithmic** representation learning algorithms for reinforcement learning in different problem settings. Learning *action* representations or abstractions, such as temporally-extended skills, has been a long-standing focus of hierarchical RL [Dietterich et al., 1998, Sutton et al., 1999, Kulkarni et al., 2016a, Nachum et al., 2018] for solving temporally-extended tasks. Recently, many algorithms have been proposed for online unsupervised skill discovery, which can reduce the cost of exploration and sample complexity of online RL algorithms. A class of methods extract temporally-extended skills by maximizing a mutual information objective [Eysenbach et al., 2018, Sharma et al., 2019, Lynch et al., 2020] or minimizing divergences [Lee et al., 2019]. Unsupervised skill discovery has been also studied in offline settings, where the goal is to pre-train useful skill representations from offline trajectories, in order to accelerate learning on downstream RL tasks [Yang and Nachum, 2021]. Such methods include OPAL [Ajay et al., 2020], SPiRL [Pertsch et al., 2020], and SkillD [Pertsch et al., 2021], which exploit a latent variable model with an autoencoder for skills acquisition; and PARROT [Singh et al., 2020], which learns a behavior prior with flow-based models. Another offline representation learning algorithm, TRAIL [Yang et al., 2021], uses a contrastive implementation of the MLE for an energy-based model to learn state-action features.

These algorithms achieve empirical performance improvements in different problem settings, such as imitation learning, policy transfer, etc. However, as far as we know, the coupling issue between exploration and representation learning has not been well handled, and there is no rigorous characterization yet for these algorithms.

Another line of research focuses on **theoretically** guaranteed representation learning in the factorizable MDP setting, either by limiting the flexibility of the models or by ignoring the practical issue of computational cost. For example, Du et al. [2019], Misra et al. [2020] considered representation learning in block MDPs, where the representation can be learned via regression. However, the corresponding representation ability is *exponentially weaker* than low-rank MDPs [Agarwal et al., 2020]. Ren et al. [2021] exploited representation from arbitrary dynamics models, but restricted the noise model to be Gaussian. On the other hand, Agarwal et al. [2020], Modi et al. [2021], Uehara et al. [2021], Zhang et al. [2022], Chen et al. [2022] provably extracted spectral features in low-rank MDPs with exploration, but their method relies on a strong computation oracle, which is difficult to implement in practice.

In contrast, the proposed SPEDER enjoys both theoretical and empirical advantages. We provide a tractable surrogate with an efficient algorithm for spectral feature learning with exploration in low-rank MDPs. We establish its sample complexity and demonstrate its superior empirical performance.

6 Experiments

We evaluate SPEDER on the dense-reward Mujoco benchmarks [Brockman et al., 2016] and sparse-reward DeepMind Control Suite tasks [Tassa et al., 2018]. In Mujoco tasks, we compare with model-based (e.g., PETS [Chua et al., 2018], ME-TRPO [Kurutach et al., 2018]) and model-free baselines (e.g., SAC [Haarnoja et al., 2018], PPO [Schulman et al., 2017]), showing strong performance compared to SoTA RL algorithms. In particular, we find that in the sparse reward DeepMind Control tasks, the optimistic SPEDER significantly outperforms the SoTA model-free RL algorithms. We also evaluate the method on offline behavioral cloning tasks in the AntMaze environment using the D4RL benchmark [Fu et al., 2020], and show comparable results to state-of-the-art representation learning methods. Additional details about the experiment setup are described in Appendix E.

Table 2: Performance on various MuJoCo control tasks. All the results are averaged across 4 random seeds and a window size of 20K. Results marked with * is adopted from MBBL [Wang et al., 2019]. SPEDER achieves strong performance compared with baselines.

		HalfCheetah	Reacher	Humanoid-ET	Pendulum	I-Pendulum
Model-Based RL	ME-TRPO*	2283.7±900.4	-13.4±5.2	72.9±8.9	177.3±1.9	-126.2±86.6
	PETS-RS*	966.9±471.6	-40.1±6.9	109.6±102.6	167.9±35.8	-12.1±25.1
	PETS-CEM*	2795.3±879.9	-12.3±5.2	110.8±90.1	167.4±53.0	-20.5±28.9
	Best MBBL	3639.0±1135.8	-4.1±0.1	1377.0±150.4	177.3±1.9	0.0±0.0
Model-Free RL	PPO*	17.2±84.4	-17.2±0.9	451.4±39.1	163.4±8.0	-40.8±21.0
	TRPO*	-12.0±85.5	-10.1±0.6	289.8±5.2	166.7±7.3	-27.6±15.8
	SAC* (3-layer)	4000.7±202.1	-6.4±0.5	1794.4±458.3	168.2±9.5	-0.2±0.1
Representation RL	DeepSF	4180.4±113.8	-16.8±3.6	168.6±5.1	168.6±5.1	-0.2±0.3
	SPEDE	4210.3±92.6	-7.2±1.1	886.9±95.2	169.5±0.6	0.0±0.0
	SPEDER	5407.9±813.0	-5.90±0.3	1774.875±129.1	167.4±3.4	0.0±0.0
		Ant-ET	Hopper-ET	S-Humanoid-ET	CartPole	Walker-ET
Model-Based RL	ME-TRPO*	42.6±21.1	1272.5±500.9	-154.9±534.3	160.1±69.1	-1609.3±657.5
	PETS-RS*	130.0±148.1	205.8±36.5	320.7±182.2	195.0±28.0	312.5±493.4
	PETS-CEM*	81.6±145.8	129.3±36.0	355.1±157.1	195.5±3.0	260.2±536.9
	Best MBBL	275.4±309.1	1272.5±500.9	1084.3±77.0	200.0±0.0	312.5±493.4
Model-Free RL	PPO*	80.1±17.3	758.0±62.0	454.3±36.7	86.5±7.8	306.1±17.2
	TRPO*	116.8±47.3	237.4±33.5	281.3±10.9	47.3±15.7	229.5±27.1
	SAC* (3-layer)	2012.7±571.3	1815.5±655.1	834.6±313.1	199.4±0.4	2216.4±678.7
Representation RL	DeepSF	768.1±44.1	548.9±253.3	533.8±154.9	194.5±5.8	165.6±127.9
	SPEDE	806.2±60.2	732.2±263.9	986.4±154.7	138.2±39.5	501.6±204.0
	SPEDER	1806.8±1488.0	2267.6±554.3	944.8±354.3	200.2±1.0	2451.5±1115.6

6.1 Online Performance with the Spectral Representation

We evaluate the proposed algorithm on the dense-reward MuJoCo benchmark from MBBL. We compare SPEDER with several model-based RL baselines (PETS [Chua et al., 2018], ME-TRPO [Kurutach et al., 2018]) and SoTA model-free RL baselines (SAC [Haarnoja et al., 2018], PPO [Schulman et al., 2017]). As a standard evaluation protocol in MBBL, we ran all the algorithms for 200K environment steps. The results are averaged across four random seeds with window size 20K.

In Table 2, we show that SPEDER achieves SoTA results among all model-based RL algorithms and significantly improves the prior baselines. We also compare the algorithm with the SoTA model-free RL method SAC. The proposed method achieves comparable or better performance in most of the tasks. Lastly, compared to two representation learning baselines (Deep SF [Kulkarni et al., 2016b] and SPEDE [Ren et al., 2021]), SPEDER also shows superior performance, which demonstrates the proposed SPEDER is able to overcome the aforementioned drawback of vanilla spectral representations.

6.2 Exploration in Sparse-Reward DeepMind Control Suite

To evaluate the exploration performance of SPEDER, we additionally run experiments in the DeepMind Control Suite. We compare the proposed method with SAC, (including a 2-layer, 3-layer and 5-layer MLP for critic network), PPO, Dreamer-v2 [Hafner et al., 2020], Deep SF [Kulkarni et al., 2016b] and Proto-RL [Yarats et al., 2021]. Since the original Dreamer and Proto-RL are designed for image-based control tasks, we adapt them to run the state-based tasks and details can be found at Appendix. E. We run all the algorithms for 200K environment steps across four random seeds with a window size of 20K. From Table 3, we see that SPEDER achieves superior performance compared to SAC using the 2-layer critic network. Compared to SAC and PPO with deeper critic networks, SPEDER has significant gain in tasks with sparse reward (e.g., walker-run-sparse and hopper-hop). Our algorithm also achieve significantly better results comparing to SAC with the same critic network size (5-layer MLP).

6.3 Imitation Learning Performance on AntMaze Navigation

We additionally experiment with using SPEDER features for downstream imitation learning, which is a framework for learning a behavior policy that mimicks a given set of expert demonstrations. We consider the challenging AntMaze navigation domain from the D4RL [Fu et al., 2020] benchmark. AntMaze (shown in Figure 3) consists of a 8-DoF quadraped robot whose task is to navigate towards a goal position in the maze environment.

We compare SPEDER to several recent methods considered to be state-of-the-art for pre-training representations from suboptimal offline data. OPAL [Ajay et al., 2020], SPiRL [Pertsch et al., 2020], and SkiLD [Pertsch et al., 2021] extract temporally-extended skills from an offline dataset to form a latent action space, which is then used to learn downstream RL tasks. TRAIL [Yang et al., 2021] pre-trains a latent action representation as part of a factored transition model, which is then used for downstream behavioral cloning. For OPAL, SPiRL, and SkiLD, we use horizons of $t = 1$ and

Table 3: Performance on various DeepMind Suite Control tasks. All the results are averaged across four random seeds and a window size of 20K. Comparing with SAC, our method achieves even better performance on sparse-reward tasks. Results are presented in mean \pm standard deviation across different random seeds.

		cheetah_run	cheetah_run_sparse	walker_run	walker_run_sparse	humanoid_run	hopper_hop
Model-Based RL	Dreamer	542.0 \pm 27.7	499.9 \pm 73.3	337.7 \pm 67.2	95.4 \pm 54.7	1.0 \pm 0.2	46.1 \pm 17.3
Model-Free RL	PPO	227.7 \pm 57.9	5.4 \pm 10.8	51.6 \pm 1.5	0.0 \pm 0.0	1.1 \pm 0.0	0.7 \pm 0.8
	SAC (2-layer)	222.2 \pm 41.0	32.4 \pm 27.8	183.0 \pm 23.4	53.5 \pm 69.3	1.3 \pm 0.1	0.4 \pm 0.5
	SAC (3-layer)	595.2 \pm 96.0	419.5 \pm 73.3	700.9 \pm 36.6	311.5 \pm 361.4	1.2 \pm 0.1	28.6 \pm 19.5
	SAC (5-layer)	566.3 \pm 123.5	364.1 \pm 242.3	716.9 \pm 35.0	276.1 \pm 319.3	8.2 \pm 13.8	31.1 \pm 31.8
Representation RL	DeepSF	295.3 \pm 43.5	0.0 \pm 0.0	27.9 \pm 2.2	0.1 \pm 0.1	0.9 \pm 0.1	0.3 \pm 0.1
	Proto RL	305.5 \pm 37.9	0.0 \pm 0.0	433.5 \pm 56.8	46.9 \pm 34.1	0.3 \pm 0.6	1.0 \pm 0.2
	SPEDER	593.7 \pm 95.1	425.5 \pm 42.8	690.4 \pm 20.5	683.2 \pm 96.0	11.5 \pm 5.4	119.8 \pm 89.6

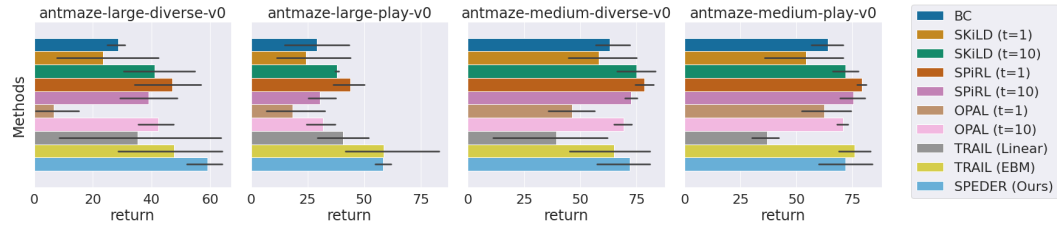


Figure 1: Average return on imitation learning tasks from D4RL AntMaze [Fu et al., 2020]. BC corresponds to behavioral cloning on the expert dataset without latent representations. All other methods pre-train representations on a suboptimal dataset, and then finetune on an expert dataset.



Figure 2: Ablation of SPEDER with vs. without normalized marginalization regularization (9).

$t = 10$ for learning temporally-extended skills. For TRAIL, we report the performance of the TRAIL energy-based model (EBM) as well as the TRAIL Linear model, which applies random Fourier features [Rahimi and Recht, 2007] to approximate a linear transition model.

For all methods, we use latent behavioral cloning as described in Section 3.2 to pre-train representations on a suboptimal dataset \mathcal{D}^{off} , then finetune on the expert dataset \mathcal{D}^{π^*} for downstream imitation learning. We also compare with baseline behavioral cloning (BC) [Pomerleau, 1998], which directly learns a policy from the expert dataset (without latent representations) by maximizing the log-likelihood objective, $\mathbb{E}_{(s,a) \sim \Pr(\mathcal{D}^{\pi^*})} [-\log \pi(a | s)]$. Following the behavioral cloning setup in [Yang et al., 2021], we use a set of 10 expert trajectories of the agent navigating from one corner of the maze to the opposite corner as the expert dataset \mathcal{D}^{π^*} . For the suboptimal dataset \mathcal{D}^{off} , we use the “diverse” or “play” datasets from D4RL [Fu et al., 2020], which consist of 1M samples of the agent navigating from different initial locations to different goal positions.

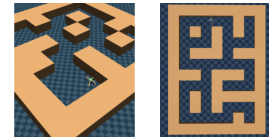


Figure 3: AntMaze navigation domains in mazes of medium (left) and large (right) sizes.

We report the average return on AntMaze tasks, and observe that SPEDER achieves comparable performance as other state-of-the-art representations on downstream imitation learning (Figure 1). We also observe that the normalized marginalization regularization (9) helps performance (Figure 2).

7 Conclusion

We have proposed a novel objective, Spectral Decomposition Representation (SPEDER), that factorizes the state-action transition kernel to obtain policy-independent spectral features. We show how to use the representations obtained with SPEDER to perform sample efficient online and offline RL, as well as imitation learning. We provide a thorough theoretical analysis of SPEDER and empirical comparisons on multiple benchmarks, demonstrating the effectiveness of SPEDER.

References

- Alekh Agarwal, Sham Kakade, Akshay Krishnamurthy, and Wen Sun. Flambe: Structural complexity and representation learning of low rank mdps. *Advances in neural information processing systems*, 33:20095–20107, 2020.
- Anurag Ajay, Aviral Kumar, Pulkit Agrawal, Sergey Levine, and Ofir Nachum. Opal: Offline primitive discovery for accelerating offline reinforcement learning. *arXiv preprint arXiv:2010.13611*, 2020.
- Ankesh Anand, Evan Racah, Sherjil Ozair, Yoshua Bengio, Marc-Alexandre Côté, and R Devon Hjelm. Unsupervised state representation learning in atari. *Advances in Neural Information Processing Systems*, 32, 2019.
- Marcin Andrychowicz, Filip Wolski, Alex Ray, Jonas Schneider, Rachel Fong, Peter Welinder, Bob McGrew, Josh Tobin, OpenAI Pieter Abbeel, and Wojciech Zaremba. Hindsight experience replay. *Advances in neural information processing systems*, 30, 2017.
- Mohammad Gheshlaghi Azar, Ian Osband, and Rémi Munos. Minimax regret bounds for reinforcement learning. In *International Conference on Machine Learning*, pages 263–272. PMLR, 2017.
- André Barreto, Will Dabney, Rémi Munos, Jonathan J Hunt, Tom Schaul, Hado P van Hasselt, and David Silver. Successor features for transfer in reinforcement learning. *Advances in neural information processing systems*, 30, 2017.
- Marc G Bellemare, Salvatore Candido, Pablo Samuel Castro, Jun Gong, Marlos C Machado, Subhodeep Moitra, Sameera S Ponda, and Ziyu Wang. Autonomous navigation of stratospheric balloons using reinforcement learning. *Nature*, 588(7836):77–82, 2020.
- Greg Brockman, Vicki Cheung, Ludwig Pettersson, Jonas Schneider, John Schulman, Jie Tang, and Wojciech Zaremba. Openai gym. *arXiv preprint arXiv:1606.01540*, 2016.
- Jinglin Chen, Aditya Modi, Akshay Krishnamurthy, Nan Jiang, and Alekh Agarwal. On the statistical efficiency of reward-free exploration in non-linear rl. *arXiv preprint arXiv:2206.10770*, 2022.
- Kurtland Chua, Roberto Calandra, Rowan McAllister, and Sergey Levine. Deep reinforcement learning in a handful of trials using probabilistic dynamics models. *Advances in neural information processing systems*, 31, 2018.
- Peter Dayan. Improving generalization for temporal difference learning: The successor representation. *Neural Computation*, 5(4):613–624, 1993.
- Thomas G Dietterich et al. The maxq method for hierarchical reinforcement learning. In *ICML*, volume 98, pages 118–126. Citeseer, 1998.
- Simon Du, Akshay Krishnamurthy, Nan Jiang, Alekh Agarwal, Miroslav Dudik, and John Langford. Provably efficient rl with rich observations via latent state decoding. In *International Conference on Machine Learning*, pages 1665–1674. PMLR, 2019.
- Yaqi Duan, Tracy Ke, and Mengdi Wang. State aggregation learning from markov transition data. *Advances in Neural Information Processing Systems*, 32, 2019.
- Benjamin Eysenbach, Abhishek Gupta, Julian Ibarz, and Sergey Levine. Diversity is all you need: Learning skills without a reward function. *arXiv preprint arXiv:1802.06070*, 2018.
- Justin Fu, Aviral Kumar, Ofir Nachum, George Tucker, and Sergey Levine. D4rl: Datasets for deep data-driven reinforcement learning, 2020.
- Clement Gehring, Leslie Pack Kaelbling, and Tomas Lozano-Perez. Adaptable replanning with compressed linear action models for learning from demonstrations. In *Conference on Robot Learning*, pages 432–442. PMLR, 2018.
- Carles Gelada, Saurabh Kumar, Jacob Buckman, Ofir Nachum, and Marc G Bellemare. Deepmdp: Learning continuous latent space models for representation learning. In *International Conference on Machine Learning*, pages 2170–2179. PMLR, 2019.

- Dibya Ghosh and Marc G Bellemare. Representations for stable off-policy reinforcement learning. In *International Conference on Machine Learning*, pages 3556–3565. PMLR, 2020.
- Dibya Ghosh, Abhishek Gupta, and Sergey Levine. Learning actionable representations with goal-conditioned policies. *arXiv preprint arXiv:1811.07819*, 2018.
- Steffen Grünewälder, Guy Lever, Luca Baldassarre, Sam Patterson, Arthur Gretton, and Massimiliano Pontil. Conditional mean embeddings as regressors. In *Proceedings of the 29th International Conference on Machine Learning, ICML’12*, page 1803–1810. Omnipress, 2012.
- Tuomas Haarnoja, Aurick Zhou, Kristian Hartikainen, George Tucker, Sehoon Ha, Jie Tan, Vikash Kumar, Henry Zhu, Abhishek Gupta, Pieter Abbeel, et al. Soft actor-critic algorithms and applications. *arXiv preprint arXiv:1812.05905*, 2018.
- Danijar Hafner, Timothy Lillicrap, Jimmy Ba, and Mohammad Norouzi. Dream to control: Learning behaviors by latent imagination. *arXiv preprint arXiv:1912.01603*, 2019.
- Danijar Hafner, Timothy Lillicrap, Mohammad Norouzi, and Jimmy Ba. Mastering atari with discrete world models. *arXiv preprint arXiv:2010.02193*, 2020.
- Max Jaderberg, Volodymyr Mnih, Wojciech Marian Czarnecki, Tom Schaul, Joel Z Leibo, David Silver, and Koray Kavukcuoglu. Reinforcement learning with unsupervised auxiliary tasks. *arXiv preprint arXiv:1611.05397*, 2016.
- Chi Jin, Zeyuan Allen-Zhu, Sebastien Bubeck, and Michael I Jordan. Is q-learning provably efficient? *Advances in neural information processing systems*, 31, 2018.
- Chi Jin, Zhuoran Yang, Zhaoran Wang, and Michael I Jordan. Provably efficient reinforcement learning with linear function approximation. In *Conference on Learning Theory*, pages 2137–2143. PMLR, 2020.
- Leslie Pack Kaelbling. Learning to achieve goals. In *IJCAI*, volume 2, pages 1094–8. Citeseer, 1993.
- Tejas D Kulkarni, Karthik Narasimhan, Ardavan Saeedi, and Josh Tenenbaum. Hierarchical deep reinforcement learning: Integrating temporal abstraction and intrinsic motivation. *Advances in neural information processing systems*, 29, 2016a.
- Tejas D Kulkarni, Ardavan Saeedi, Simanta Gautam, and Samuel J Gershman. Deep successor reinforcement learning. *arXiv preprint arXiv:1606.02396*, 2016b.
- Thanard Kurutach, Ignasi Clavera, Yan Duan, Aviv Tamar, and Pieter Abbeel. Model-ensemble trust-region policy optimization. *arXiv preprint arXiv:1802.10592*, 2018.
- Misha Laskin, Kimin Lee, Adam Stooke, Lerrel Pinto, Pieter Abbeel, and Aravind Srinivas. Reinforcement learning with augmented data. *Advances in Neural Information Processing Systems*, 33: 19884–19895, 2020.
- Lisa Lee, Benjamin Eysenbach, Emilio Parisotto, Eric Xing, Sergey Levine, and Ruslan Salakhutdinov. Efficient exploration via state marginal matching. *arXiv preprint arXiv:1906.05274*, 2019.
- Lisa Lee, Ben Eysenbach, Russ R Salakhutdinov, Shixiang Shane Gu, and Chelsea Finn. Weakly-supervised reinforcement learning for controllable behavior. *Advances in Neural Information Processing Systems*, 33:2661–2673, 2020.
- Sergey Levine, Chelsea Finn, Trevor Darrell, and Pieter Abbeel. End-to-end training of deep visuomotor policies. *The Journal of Machine Learning Research*, 17(1):1334–1373, 2016.
- Corey Lynch, Mohi Khansari, Ted Xiao, Vikash Kumar, Jonathan Tompson, Sergey Levine, and Pierre Sermanet. Learning latent plans from play. In *Conference on robot learning*, pages 1113–1132. PMLR, 2020.
- Marlos C Machado, Marc G Bellemare, and Michael Bowling. A laplacian framework for option discovery in reinforcement learning. In *International Conference on Machine Learning*, pages 2295–2304. PMLR, 2017.

- Marlos C. Machado, Clemens Rosenbaum, Xiaoxiao Guo, Miao Liu, Gerald Tesauro, and Murray Campbell. Eigenoption discovery through the deep successor representation. In *International Conference on Learning Representations*, 2018. URL <https://openreview.net/forum?id=Bk8ZcAxR->.
- Sridhar Mahadevan and Mauro Maggioni. Proto-value functions: A laplacian framework for learning representation and control in markov decision processes. *Journal of Machine Learning Research*, 8(10), 2007.
- Dipendra Misra, Mikael Henaff, Akshay Krishnamurthy, and John Langford. Kinematic state abstraction and provably efficient rich-observation reinforcement learning. In *International conference on machine learning*, pages 6961–6971. PMLR, 2020.
- Volodymyr Mnih, Koray Kavukcuoglu, David Silver, Andrei A Rusu, Joel Veness, Marc G Bellemare, Alex Graves, Martin Riedmiller, Andreas K Fidjeland, Georg Ostrovski, et al. Human-level control through deep reinforcement learning. *nature*, 518(7540):529–533, 2015.
- Aditya Modi, Jinglin Chen, Akshay Krishnamurthy, Nan Jiang, and Alekh Agarwal. Model-free representation learning and exploration in low-rank mdps. *arXiv preprint arXiv:2102.07035*, 2021.
- Ofir Nachum, Shixiang Shane Gu, Honglak Lee, and Sergey Levine. Data-efficient hierarchical reinforcement learning. *Advances in neural information processing systems*, 31, 2018.
- Ashvin V Nair, Vitchyr Pong, Murtaza Dalal, Shikhar Bahl, Steven Lin, and Sergey Levine. Visual reinforcement learning with imagined goals. *Advances in neural information processing systems*, 31, 2018.
- Junhyuk Oh, Satinder Singh, and Honglak Lee. Value prediction network. *Advances in neural information processing systems*, 30, 2017.
- Aaron van den Oord, Yazhe Li, and Oriol Vinyals. Representation learning with contrastive predictive coding. *arXiv preprint arXiv:1807.03748*, 2018.
- Ronald Parr, Lihong Li, Gavin Taylor, Christopher Painter-Wakefield, and Michael L Littman. An analysis of linear models, linear value-function approximation, and feature selection for reinforcement learning. In *Proceedings of the 25th international conference on Machine learning*, pages 752–759, 2008.
- Deepak Pathak, Pulkit Agrawal, Alexei A Efros, and Trevor Darrell. Curiosity-driven exploration by self-supervised prediction. In *International conference on machine learning*, pages 2778–2787. PMLR, 2017.
- Karl Pertsch, Youngwoon Lee, and Joseph J Lim. Accelerating reinforcement learning with learned skill priors. *arXiv preprint arXiv:2010.11944*, 2020.
- Karl Pertsch, Youngwoon Lee, Yue Wu, and Joseph J Lim. Guided reinforcement learning with learned skills. *arXiv preprint arXiv:2107.10253*, 2021.
- Marek Petrik. An analysis of laplacian methods for value function approximation in mdps. In *Proceedings of the 20th International Joint Conference on Artificial Intelligence, IJCAI’07*, page 2574–2579, San Francisco, CA, USA, 2007. Morgan Kaufmann Publishers Inc.
- D Pomerleau. An autonomous land vehicle in a neural network. *Advances in Neural Information Processing Systems*, 1, 1998.
- Vitchyr H Pong, Murtaza Dalal, Steven Lin, Ashvin Nair, Shikhar Bahl, and Sergey Levine. Skew-fit: State-covering self-supervised reinforcement learning. *arXiv preprint arXiv:1903.03698*, 2019.
- Sébastien Racanière, Théophane Weber, David Reichert, Lars Buesing, Arthur Guez, Danilo Jimenez Rezende, Adrià Puigdomènech Badia, Oriol Vinyals, Nicolas Heess, Yujia Li, et al. Imagination-augmented agents for deep reinforcement learning. *Advances in neural information processing systems*, 30, 2017.
- Ali Rahimi and Benjamin Recht. Random features for large-scale kernel machines. *Advances in neural information processing systems*, 20, 2007.

- Prajit Ramachandran, Barret Zoph, and Quoc V Le. Searching for activation functions. *arXiv preprint arXiv:1710.05941*, 2017.
- Tongzheng Ren, Tianjun Zhang, Csaba Szepesvári, and Bo Dai. A free lunch from the noise: Provable and practical exploration for representation learning. *arXiv preprint arXiv:2111.11485*, 2021.
- Tom Schaul, Daniel Horgan, Karol Gregor, and David Silver. Universal value function approximators. In *International conference on machine learning*, pages 1312–1320. PMLR, 2015.
- John Schulman, Filip Wolski, Prafulla Dhariwal, Alec Radford, and Oleg Klimov. Proximal policy optimization algorithms. *arXiv preprint arXiv:1707.06347*, 2017.
- Pierre Sermanet, Corey Lynch, Yevgen Chebotar, Jasmine Hsu, Eric Jang, Stefan Schaal, Sergey Levine, and Google Brain. Time-contrastive networks: Self-supervised learning from video. In *2018 IEEE international conference on robotics and automation (ICRA)*, pages 1134–1141. IEEE, 2018.
- Archit Sharma, Shixiang Gu, Sergey Levine, Vikash Kumar, and Karol Hausman. Dynamics-aware unsupervised discovery of skills. *arXiv preprint arXiv:1907.01657*, 2019.
- David Silver, Julian Schrittwieser, Karen Simonyan, Ioannis Antonoglou, Aja Huang, Arthur Guez, Thomas Hubert, Lucas Baker, Matthew Lai, Adrian Bolton, et al. Mastering the game of go without human knowledge. *nature*, 550(7676):354–359, 2017.
- David Silver, Thomas Hubert, Julian Schrittwieser, Ioannis Antonoglou, Matthew Lai, Arthur Guez, Marc Lanctot, Laurent Sifre, Dharmashan Kumaran, Thore Graepel, et al. A general reinforcement learning algorithm that masters chess, shogi, and go through self-play. *Science*, 362(6419): 1140–1144, 2018.
- Avi Singh, Huihan Liu, Gaoyue Zhou, Albert Yu, Nicholas Rhinehart, and Sergey Levine. Parrot: Data-driven behavioral priors for reinforcement learning. *arXiv preprint arXiv:2011.10024*, 2020.
- Aravind Srinivas, Michael Laskin, and Pieter Abbeel. Curl: Contrastive unsupervised representations for reinforcement learning. *arXiv preprint arXiv:2004.04136*, 2020.
- Adam Stooke, Kimin Lee, Pieter Abbeel, and Michael Laskin. Decoupling representation learning from reinforcement learning. In *International Conference on Machine Learning*, pages 9870–9879. PMLR, 2021.
- Richard S Sutton, Doina Precup, and Satinder Singh. Between mdps and semi-mdps: A framework for temporal abstraction in reinforcement learning. *Artificial intelligence*, 112(1-2):181–211, 1999.
- Yuval Tassa, Yotam Doron, Alistair Muldal, Tom Erez, Yazhe Li, Diego de Las Casas, David Budden, Abbas Abdolmaleki, Josh Merel, Andrew Lefrancq, et al. Deepmind control suite. *arXiv preprint arXiv:1801.00690*, 2018.
- Ahmed Touati and Yann Ollivier. Learning one representation to optimize all rewards. *Advances in Neural Information Processing Systems*, 34:13–23, 2021.
- Masatoshi Uehara, Xuezhou Zhang, and Wen Sun. Representation learning for online and offline rl in low-rank mdps. 2021.
- Tingwu Wang, Xuchan Bao, Ignasi Clavera, Jerrick Hoang, Yeming Wen, Eric Langlois, Shunshi Zhang, Guodong Zhang, Pieter Abbeel, and Jimmy Ba. Benchmarking model-based reinforcement learning. *arXiv preprint arXiv:1907.02057*, 2019.
- Manuel Watter, Jost Springenberg, Joschka Boedecker, and Martin Riedmiller. Embed to control: A locally linear latent dynamics model for control from raw images. *Advances in neural information processing systems*, 28, 2015.
- Yifan Wu, George Tucker, and Ofir Nachum. The laplacian in rl: Learning representations with efficient approximations. In *International Conference on Learning Representations*, 2018.

- Chenjun Xiao, Bo Dai, Jincheng Mei, Oscar A Ramirez, Ramki Gummadi, Chris Harris, and Dale Schuurmans. Understanding and leveraging overparameterization in recursive value estimation. In *International Conference on Learning Representations*, 2021.
- Mengjiao Yang and Ofir Nachum. Representation matters: Offline pretraining for sequential decision making. In *International Conference on Machine Learning*, pages 11784–11794. PMLR, 2021.
- Mengjiao Yang, Sergey Levine, and Ofir Nachum. Trail: Near-optimal imitation learning with suboptimal data. *arXiv preprint arXiv:2110.14770*, 2021.
- Hengshuai Yao and Csaba Szepesvári. Approximate policy iteration with linear action models. In *Proceedings of the AAAI Conference on Artificial Intelligence*, volume 26, pages 1212–1218, 2012.
- Denis Yarats, Rob Fergus, Alessandro Lazaric, and Lerrel Pinto. Reinforcement learning with prototypical representations. In *International Conference on Machine Learning*, pages 11920–11931. PMLR, 2021.
- Amy Zhang, Rowan McAllister, Roberto Calandra, Yarin Gal, and Sergey Levine. Learning invariant representations for reinforcement learning without reconstruction. *arXiv preprint arXiv:2006.10742*, 2020.
- Anru Zhang and Mengdi Wang. Spectral state compression of markov processes. *IEEE transactions on information theory*, 66(5):3202–3231, 2019.
- Tong Zhang. Information-theoretic upper and lower bounds for statistical estimation. *IEEE Transactions on Information Theory*, 52(4):1307–1321, 2006.
- Xuezhou Zhang, Yuda Song, Masatoshi Uehara, Mengdi Wang, Alekh Agarwal, and Wen Sun. Efficient reinforcement learning in block mdps: A model-free representation learning approach. In *International Conference on Machine Learning*, pages 26517–26547. PMLR, 2022.

Checklist

The checklist follows the references. Please read the checklist guidelines carefully for information on how to answer these questions. For each question, change the default **[TODO]** to **[Yes]**, **[No]**, or **[N/A]**. You are strongly encouraged to include a **justification to your answer**, either by referencing the appropriate section of your paper or providing a brief inline description. For example:

- Did you include the license to the code and datasets? **[Yes]** See Section ??.
- Did you include the license to the code and datasets? **[No]** The code and the data are proprietary.
- Did you include the license to the code and datasets? **[N/A]**

Please do not modify the questions and only use the provided macros for your answers. Note that the Checklist section does not count towards the page limit. In your paper, please delete this instructions block and only keep the Checklist section heading above along with the questions/answers below.

1. For all authors...
 - (a) Do the main claims made in the abstract and introduction accurately reflect the paper’s contributions and scope? **[Yes]**
 - (b) Did you describe the limitations of your work? **[Yes]**
 - (c) Did you discuss any potential negative societal impacts of your work? **[N/A]**
 - (d) Have you read the ethics review guidelines and ensured that your paper conforms to them? **[Yes]**
2. If you are including theoretical results...
 - (a) Did you state the full set of assumptions of all theoretical results? **[Yes]**
 - (b) Did you include complete proofs of all theoretical results? **[Yes]**
3. If you ran experiments...

- (a) Did you include the code, data, and instructions needed to reproduce the main experimental results (either in the supplemental material or as a URL)? [\[Yes\]](#)
 - (b) Did you specify all the training details (e.g., data splits, hyperparameters, how they were chosen)? [\[Yes\]](#)
 - (c) Did you report error bars (e.g., with respect to the random seed after running experiments multiple times)? [\[Yes\]](#)
 - (d) Did you include the total amount of compute and the type of resources used (e.g., type of GPUs, internal cluster, or cloud provider)? [\[Yes\]](#)
4. If you are using existing assets (e.g., code, data, models) or curating/releasing new assets...
- (a) If your work uses existing assets, did you cite the creators? [\[Yes\]](#)
 - (b) Did you mention the license of the assets? [\[Yes\]](#)
 - (c) Did you include any new assets either in the supplemental material or as a URL? [\[N/A\]](#)
 - (d) Did you discuss whether and how consent was obtained from people whose data you're using/curating? [\[N/A\]](#)
 - (e) Did you discuss whether the data you are using/curating contains personally identifiable information or offensive content? [\[N/A\]](#)
5. If you used crowdsourcing or conducted research with human subjects...
- (a) Did you include the full text of instructions given to participants and screenshots, if applicable? [\[N/A\]](#)
 - (b) Did you describe any potential participant risks, with links to Institutional Review Board (IRB) approvals, if applicable? [\[N/A\]](#)
 - (c) Did you include the estimated hourly wage paid to participants and the total amount spent on participant compensation? [\[N/A\]](#)

A More Related Work

Representation learning in RL has attracted more attention in recent years. Within model-based RL (MBRL), many methods for learning representations of the reward and the dynamics have been proposed. Several recent MBRL methods learn latent state representations to be used for planning in latent space as a way to improve model-based policy optimization [Oh et al., 2017, Silver et al., 2018, Racanière et al., 2017, Hafner et al., 2019].

Beyond MBRL, there also exist many algorithms for learning useful state representations to accelerate RL. For example, recent works have introduced unsupervised auxiliary losses to significantly improve RL performance [Pathak et al., 2017, Oord et al., 2018, Laskin et al., 2020, Jaderberg et al., 2016]. Contrastive losses [Oord et al., 2018, Anand et al., 2019, Srinivas et al., 2020, Stooke et al., 2021], which encourage similar states to be closer in embedding space, where the notion of similarity is usually defined in terms of temporal distance [Anand et al., 2019, Sermanet et al., 2018] or image-based data augmentations [Srinivas et al., 2020], also show promising performance. Within goal-conditioned RL [Kaelbling, 1993, Schaul et al., 2015, Andrychowicz et al., 2017], various representation learning algorithms have been proposed to handle high-dimensional observation and goal spaces, such as using a variational autoencoder [Nair et al., 2018, Pong et al., 2019], or representations that explicitly capture useful information for control, while ignoring irrelevant factors of variation in the observation [Ghosh et al., 2018, Lee et al., 2020].

Beyond these representations on the state space, there are other kinds of representations that are designed for specific tasks. For example, Touati and Ollivier [2021] proposed to deal with the reward transfer task by learning a reward-dependent feature $F(s, a, r)$ such that the greedy policy with respect to $F(s, a, r)^\top r$ is optimal under r .

B Algorithm for Offline Policy Optimization

For completeness, we include the algorithm for offline policy optimization with SPEDER here.

Algorithm 2 Offline Policy Optimization with SPEDER

- 1: **Input:** Regularizer λ , Parameter α , Model class \mathcal{F} , Dataset \mathcal{D} sampled from the stationary distribution of the behavior policy π_b .
- 2: Learn representation $\hat{\phi}(s, a)$ with \mathcal{D} via (8).
- 3: Set the empirical covariance matrix

$$\hat{\Sigma} = \sum_{(s,a) \in \mathcal{D}} \hat{\phi}(s, a) \hat{\phi}(s, a)^\top + \lambda I.$$

- 4: Set the reward penalty: $\hat{b}(s, a) = \alpha \sqrt{\hat{\phi}(s, a)^\top \hat{\Sigma}^{-1} \hat{\phi}(s, a)}$.
 - 5: Solve $\hat{\pi} = \arg \max_{\pi} V_{\hat{P}, r - \hat{b}}^\pi$.
 - 6: **Return** $\hat{\pi}$
-

C Proof Details

C.1 Non-asymptotic Generalization Bound

In this subsection, we consider the non-asymptotic generalization bound for the ℓ_2 minimization, which is necessary for the proof of series of key lemmas (Lemma 7 and Lemma 15) that are used in the PAC guarantee of the online and offline reinforcement learning. For simplicity, we denote the instance space as \mathcal{X} and the target space as \mathcal{Y} , and we want to estimate the conditional density $p(y|x) = f^*(x, y)$. Assume we are given a function class $\mathcal{F} : (\mathcal{X} \times \mathcal{Y}) \rightarrow \mathbb{R}$ with $f^* \in \mathcal{F}$, as well as the data $\mathcal{D} := \{(x_i, y_i)\}_{i=1}^n$, where $x_i \sim \mathcal{D}_i(x_{1:i-1}, y_{1:i-1})$, $y_i \sim p(\cdot|x_i)$ and \mathcal{D}_i is some data generating process that depends on the previous samples (a.k.a a martingale process). We define the tangent sequence $\mathcal{D}' := \{(x'_i, y'_i)\}$ where $x'_i \sim \mathcal{D}_i(x_{1:i-1}, y_{1:i-1})$ and $y'_i \sim p(\cdot|x'_i)$. Consider the

estimator obtained by following minimization problem:

$$\hat{f} = \arg \min_{f \in \mathcal{F}} \left\{ \sum_{i=1}^n -2f(x_i, y_i) + \sum_{i=1}^n \left(\sum_{y \in \mathcal{Y}} f^2(x_i, y) \right) \right\}, \quad (11)$$

where the summation over the counting measure of \mathcal{Y} for discrete case can be replaced by the integration over the Lebesgue measure of \mathcal{Y} for continuous case. We first prove the following decoupling inequality motivated by Lemma 24 of [Agarwal et al., 2020].

Lemma 4. Let $L(f, \mathcal{D}) = \sum_{i=1}^n \ell(f, (x_i, y_i))$, \mathcal{D}' is a tangent sequence of \mathcal{D} and $\hat{f}(\mathcal{D})$ be any estimator taking random variable \mathcal{D} as input with range \mathcal{F} . Then

$$\mathbb{E}_{\mathcal{D}} \left[\exp \left(-L(\hat{f}(\mathcal{D}), \mathcal{D}) - \log \mathbb{E}_{\mathcal{D}'} [\exp(-L(\hat{f}(\mathcal{D}), \mathcal{D}'))] - \log |\mathcal{F}| \right) \right] \leq 1.$$

Proof. Let π be the uniform distribution over \mathcal{F} and $g : \mathcal{F} \rightarrow \mathbb{R}$ be any function. Define the following probability measure over \mathcal{F} : $\mu(f) = \frac{\exp g(f)}{\sum_{f \in \mathcal{F}} \exp(g(f))}$. Then for any probability distribution $\hat{\pi}$ over \mathcal{F} , we have:

$$\begin{aligned} 0 &\leq \text{KL}(\hat{\pi} \parallel \mu) \\ &= \sum_{f \in \mathcal{F}} \hat{\pi}(f) \log \frac{\hat{\pi}(f)}{\mu(f)} \\ &= \sum_{f \in \mathcal{F}} [\hat{\pi}(f) \log \hat{\pi}(f) - \hat{\pi}(f)g(f)] + \log \sum_{f \in \mathcal{F}} \exp(g(f)) \\ &= \sum_{f \in \mathcal{F}} [\hat{\pi}(f) \log \hat{\pi}(f) + \hat{\pi}(f) \log |\mathcal{F}|] - \sum_{f \in \mathcal{F}} \hat{\pi}(f)g(f) + \log \mathbb{E}_{f \sim \pi} \exp(g(f)) \\ &= \text{KL}(\hat{\pi} \parallel \pi) - \sum_{f \in \mathcal{F}} \hat{\pi}(f)g(f) + \log \mathbb{E}_{f \sim \pi} \exp(g(f)) \\ &\leq \log |\mathcal{F}| - \sum_{f \in \mathcal{F}} \hat{\pi}(f)g(f) + \log \mathbb{E}_{f \sim \pi} \exp(g(f)). \end{aligned}$$

Re-arranging, we have that

$$\sum_f \hat{\pi}(f)g(f) - \log |\mathcal{F}| \leq \log \mathbb{E}_{f \sim \pi} \exp(g(f)).$$

Take $g = -L(f, \mathcal{D}) - \log \mathbb{E}_{\mathcal{D}'} [\exp(-L(f, \mathcal{D}'))]$, $\hat{\pi}(f) = \mathbf{1}_{\hat{f}(\mathcal{D})}$, we obtain that for any \mathcal{D} ,

$$-L(\hat{f}(\mathcal{D}), \mathcal{D}) - \log \mathbb{E}_{\mathcal{D}'} [\exp(-L(\hat{f}(\mathcal{D}), \mathcal{D}'))] - \log |\mathcal{F}| \leq \log \mathbb{E}_{f \sim \pi} \frac{\exp(-L(\hat{f}(\mathcal{D}), \mathcal{D}))}{\mathbb{E}_{\mathcal{D}'} [\exp(-L(\hat{f}(\mathcal{D}), \mathcal{D}'))]}.$$

We exponentiate both sides and take the expectation over \mathcal{D} , which gives

$$\mathbb{E}_{\mathcal{D}} \left[\exp \left(-L(\hat{f}(\mathcal{D}), \mathcal{D}) - \log \mathbb{E}_{\mathcal{D}'} [\exp(-L(\hat{f}(\mathcal{D}), \mathcal{D}'))] - \log |\mathcal{F}| \right) \right] \leq \mathbb{E}_{f \sim \pi} \mathbb{E}_{\mathcal{D}} \frac{\exp(-L(\hat{f}(\mathcal{D}), \mathcal{D}))}{\mathbb{E}_{\mathcal{D}'} [\exp(-L(\hat{f}(\mathcal{D}), \mathcal{D}')) | \mathcal{D}] }.$$

Note that, conditioned on \mathcal{D} , the samples in the tangent sequence \mathcal{D}' are independent, which leads to

$$\mathbb{E}_{\mathcal{D}'} \exp \left[-L(\hat{f}(\mathcal{D}), \mathcal{D}') | \mathcal{D} \right] = \prod_{i=1}^n \exp \left(\mathbb{E}_{(x_i, y_i) \sim \mathcal{D}_i} [-l(f, (x_i, y_i))] \right).$$

As a result, we can peel off terms from n down to 1 and cancel out terms in the numerator. Hence, we have

$$\mathbb{E}_{\mathcal{D}} \left[-\exp \left(L(\hat{f}(\mathcal{D}), \mathcal{D}) - \log \mathbb{E}_{\mathcal{D}'} [\exp(-L(\hat{f}(\mathcal{D}), \mathcal{D}'))] - \log |\mathcal{F}| \right) \right] \leq 1,$$

which concludes the proof. \square

Theorem 5. Assume $|\mathcal{F}| < \infty$, $f^* \in \mathcal{F}$ and $\|f(x, y)\|_{\infty} \leq C$, $\forall f \in \mathcal{F}$. Then with probability at least $1 - \delta$, we have

$$\sum_{i=1}^n \mathbb{E}_{x_i \sim \mathcal{D}_i} \|f^* - f\|_2^2 \leq C' \log |\mathcal{F}| / \delta,$$

where C' only depends on C .

With Chernoff's method, we have that

$$-\log \mathbb{E}_{\mathcal{D}'} \left[\exp \left(-L(\hat{f}(\mathcal{D}), \mathcal{D}') \right) \right] \leq L(\hat{f}(\mathcal{D}), \mathcal{D}) + \log |\mathcal{F}| + \log 1/\delta.$$

Take

$$l(f, (x_i, y_i)) = 2(f^*(x_i, y_i) - f(x_i, y_i)) + \sum_{y \in \mathcal{Y}} (f(x_i, y)^2 - f^*(x_i, y)^2),$$

and

$$L(f, \mathcal{D}) = \rho \left(\sum_{i=1}^n 2(f^*(x_i, y_i) - f(x_i, y_i)) + \sum_{i=1}^n \sum_{y \in \mathcal{Y}} (f(x_i, y)^2 - f^*(x_i, y)^2) \right),$$

where $\rho > 0$ is a constant to determine later. As $\hat{f}(\mathcal{D})$ is obtained by minimizing $L(f, \mathcal{D})$, and $f^* \in \mathcal{F}$, we have $L(\hat{f}(\mathcal{D}), \mathcal{D}) \leq L(f^*, \mathcal{D}) \leq 0$. Furthermore, as \mathcal{D}' is the tangent sequence of \mathcal{D} , direct computation shows

$$-\log \mathbb{E}_{\mathcal{D}'} \left[\exp \left(-L(\hat{f}(\mathcal{D}), \mathcal{D}') \right) \right] \leq \log \frac{|\mathcal{F}|}{\delta}.$$

We now relate the term $-\log \mathbb{E}_{\mathcal{D}'} \left[\exp \left(-L(\hat{f}(\mathcal{D}), \mathcal{D}') \right) \right]$ with our target $\sum_{i=1}^n \mathbb{E}_{x_i \sim \mathcal{D}_i} \|\hat{f}(x_i, \cdot) - f^*(x_i, \cdot)\|_2^2$ using the method introduced in [Zhang \[2006\]](#).

Note that $\sum_{y \in \mathcal{Y}} f(x, y) = 1$, as $\|f\|_\infty \leq C$, with a straightforward application of Hölder's inequality, we have that $\sum_{y \in \mathcal{Y}} f(x, y)^2 \leq C$. We then consider the term

$$\begin{aligned} & \mathbb{E}_{y_i \sim f^*(x_i, y)} [l(f, (x_i, y_i))^2] + \mathbb{E}_{y_i \sim f(x_i, y)} [l(f, (x_i, y_i))^2] \\ &= 4 \sum_{y \in \mathcal{Y}} [(f(x_i, y) + f^*(x_i, y))(f(x_i, y) - f^*(x_i, y))^2] - 3 \left(\sum_{y \in \mathcal{Y}} (f^*(x_i, y)^2 - f(x_i, y)^2) \right)^2 \\ &\leq \sum_{y \in \mathcal{Y}} ((f(x_i, y) - f^*(x_i, y))^2) \left(8C + 3 \sum_{y \in \mathcal{Y}} (f(x_i, y) + f^*(x_i, y))^2 \right) \\ &\leq 20C \sum_{y \in \mathcal{Y}} ((f(x_i, y) - f^*(x_i, y))^2) \\ &= 20C \mathbb{E}_{y_i \sim f^*(x_i, y)} [l(f, (x_i, y_i))]^2. \end{aligned}$$

As $\mathbb{E}_{y_i \sim f(x_i, y)} [l(f, (x_i, y_i))^2] \geq 0$, we can conclude that

$$\mathbb{E}_{y_i \sim f^*(x_i, y)} [l(f, (x_i, y_i))^2] \leq (20C \mathbb{E}_{y_i \sim f^*(x_i, y)} [l(f, (x_i, y_i))])^2.$$

Furthermore, it is straightforward to see $|l(f, (x_i, y_i))| \leq 3C$. With the last bound in Proposition 1.2 in [Zhang \[2006\]](#), we have that

$$\begin{aligned} & \log \mathbb{E}_{\mathcal{D}'} \left[\exp \left(-L(\hat{f}(\mathcal{D}), \mathcal{D}') \right) \right] \\ &= \sum_{i=1}^n \log \mathbb{E}_{(x_i, y_i) \sim \mathcal{D}_i} [\exp(-\rho l(f, (x_i, y_i)))] \\ &\leq -\rho \sum_{i=1}^n \mathbb{E}_{(x_i, y_i) \sim \mathcal{D}_i} [l(f, (x_i, y_i))] + \frac{\exp(3\rho C) - 3\rho C - 1}{9C^2} \mathbb{E}_{(x_i, y_i) \sim \mathcal{D}_i} [l(f, (x_i, y_i))^2] \\ &\leq -\left(\rho - \frac{20(\exp(3\rho C) - 3\rho C - 1)}{9C} \right) \sum_{i=1}^n \mathbb{E}_{(x_i, y_i) \sim \mathcal{D}_i} \|\hat{f}(x_i, \cdot) - f^*(x_i, \cdot)\|_2^2. \end{aligned}$$

As $\exp(x) - x - 1 \approx 0.5x^2$ as $x \rightarrow 0$, we know there exists sufficiently small ρ that only depends on C , such that $9\rho C > 20(\exp(3\rho C) - 3\rho C - 1)$. Hence, we know that,

$$\mathbb{E}_{(x_i, y_i) \sim \mathcal{D}_i} \|\hat{f}(x_i, \cdot) - f^*(x_i, \cdot)\|_2^2 \leq \frac{9C}{9\rho C - 20(\exp(3\rho C) - 3\rho C - 1)} \log \frac{|\mathcal{F}|}{\delta}.$$

Compared with the MLE guarantee For discrete domain, as L_2 norm is always bounded by L_1 norm, our guarantee is weaker than the guarantee of MLE used in [Agarwal et al., 2020, Uehara et al., 2021]. However, for general cases, L_1 and L_2 does not imply each other, and hence we cannot directly compare our theoretical guarantee with the MLE guarantee. Nevertheless, our method is easier to optimize compared to the MLE, which makes it a preferable practical choice.

C.2 PAC bounds for Online Reinforcement Learning

Before we start, we first state some basic properties of MDP that can be obtained from the definition of the related terms. For the state visitation distribution, a straightforward computation shows that

$$d_P^\pi(s) = (1 - \gamma)\rho(s) + \gamma \mathbb{E}_{\tilde{s} \sim d_P^\pi, \tilde{a} \sim \pi(\cdot|\tilde{s})} P(s|\tilde{s}, \tilde{a}).$$

Meanwhile, we have that

$$V_{P,r}^\pi = \frac{1}{1 - \gamma} \mathbb{E}_{s \sim d_P^\pi, a \sim \pi(\cdot|s)} [r(s, a)].$$

For now, we assume $\hat{P}_n(\cdot, \cdot)$ is a valid probability measure, $P \in \mathcal{F}$, and the following two inequalities hold $\forall n \in \mathbb{N}^+$ with probability at least $1 - \delta$:

$$\begin{aligned} \mathbb{E}_{s \sim \rho_n, a \sim \mathcal{U}(\mathcal{A})} \|\hat{P}_n(\cdot|s, a) - P(\cdot|s, a)\|_2^2 &\leq \zeta_n \\ \mathbb{E}_{s \sim \rho'_n, a \sim \mathcal{U}(\mathcal{A})} \|\hat{P}_n(\cdot|s, a) - P(\cdot|s, a)\|_2^2 &\leq \zeta_n \end{aligned}$$

Proof Sketch Our proof is organized as follows:

- Based on Theorem 5, we prove a one-step back inequality for the learned model (Lemma 7), which is further used to show the optimistic, *i.e.*, the policy planning on the learned model with the additional bonus upper bound the optimal value up to some error term (Lemma 9).
- We then bound the cumulative regret of the adaptive chosen policy (Lemma 13) based on the established optimistic, and further exploit a one-step back inequality for the true model (Lemma 10) and standard elliptical potential lemma (Lemma 20).
- With standard regret to PAC conversion, we obtain the final PAC guarantee (Theorem 14).

We first state the following basic property for the value function:

Lemma 6 (L_2 norm of $V_{P,r}^\pi$). *For any policy π , we have that*

$$\|V_{P,r}^\pi\|_2 \leq \sqrt{2d \left(1 + \frac{d\gamma^2}{(1 - \gamma)^2}\right)} \lesssim \frac{d}{1 - \gamma}$$

Proof. From the properties of low-rank MDP, we know there exists w^π , $\|w^\pi\|_2 \leq \frac{\sqrt{d}}{1 - \gamma}$ and $Q_{P,r}^\pi(s, a) = \phi^*(s, a)^\top w_h^\pi$. Then we have

$$\begin{aligned} \|V_{P,r}^\pi\|_2^2 &= \int_{\mathcal{S}} V^\pi(s)^2 ds \\ &= \int_{\mathcal{S}} \left(\int_{\mathcal{A}} \pi(a|s) (r(s, a) + \gamma Q_{P,r}^\pi(s, a)) da \right)^2 ds \\ &\leq \int_{\mathcal{S}} \left(\int_{\mathcal{A}} r(s, a) + \gamma Q_{P,r}^\pi(s, a) da \right)^2 ds \\ &\leq 2 \int_{\mathcal{S}} \left[\int_{\mathcal{A}} r(s, a) da \right]^2 ds + 2\gamma^2 \left[\int_{\mathcal{A}} Q_{P,r}^\pi(s, a) da \right]^2 ds \\ &\leq 2d + \frac{2d\gamma^2}{(1 - \gamma)^2} \int_{\mathcal{S}} \left[\int_{\mathcal{A}} \|\phi^*(s, a)\|_2 da \right]^2 ds \\ &\leq 2d \left(1 + \frac{d\gamma^2}{(1 - \gamma)^2} \right) \\ &\lesssim \frac{d^2}{(1 - \gamma)^2}, \end{aligned}$$

which concludes the proof. \square

Before we proceed to the proof, we first define the following terms. Let $\rho_n(s) = \frac{1}{n} \sum_{i=1}^n d_{P^*}^{\pi_i}(s)$. With slightly abuse of notation, we also use $\rho_n(s, a) = \frac{1}{n} \sum_{i=1}^n d_{P^*}^{\pi_i}(s, a)$, and use ρ'_n to denote the marginal distribution of s' for the triple $(s, a, s') \sim \rho_n(s) \mathcal{U}(a) P^*(s'|s, a)$. For notation simplicity, we denote

$$\begin{aligned}\Sigma_{\rho_n \times \mathcal{U}(\mathcal{A}), \phi} &= n \mathbb{E}_{s \sim \rho_n, a \sim \mathcal{U}(\mathcal{A})} [\phi(s, a) \phi(s, a)^\top] + \lambda_n I, \\ \Sigma_{\rho_n, \phi} &= n \mathbb{E}_{(s, a) \sim \rho_n} [\phi(s, a) \phi(s, a)^\top] + \lambda_n I, \\ \widehat{\Sigma}_{n, \phi} &= n \mathbb{E}_{(s, a) \sim \mathcal{D}_n} [\phi(s, a) \phi(s, a)^\top] + \lambda_n I.\end{aligned}$$

The following lemmas will be helpful when we demonstrate the effectiveness of our bonus:

Lemma 7 (One-step back inequality for the learned model). *Assume $g : \mathcal{S} \times \mathcal{A} \rightarrow \mathbb{R}$ satisfies that $\|g\|_\infty \leq B_\infty$, $\|\int_{\mathcal{A}} g(\cdot, a) da\|_2 \leq B_2$, then we have that*

$$\begin{aligned}\left| \mathbb{E}_{(s, a) \sim d_{\widehat{P}_n}^\pi} \{g(s, a)\} \right| &\leq \sqrt{(1 - \gamma) |\mathcal{A}| \mathbb{E}_{s \sim \rho_n, a \sim \mathcal{U}(\mathcal{A})} \{g^2(s, a)\}} \\ &+ \gamma \sqrt{n |\mathcal{A}| \mathbb{E}_{s \sim \rho'_n, a \sim \mathcal{U}(\mathcal{A})} \{g^2(s, a)\} + B_2^2 n \zeta_n + \lambda_n B_\infty^2 d \cdot \mathbb{E}_{(\tilde{s}, \tilde{a}) \sim d_{\widehat{P}_n}^\pi} \left[\left\| \widehat{\phi}_n(\tilde{s}, \tilde{a}) \right\|_{\Sigma_{\rho_n \times \mathcal{U}, \widehat{\phi}_n}^{-1}}^2 \right]}.\end{aligned}$$

Proof. Note that

$$\mathbb{E}_{(s, a) \sim d_{\widehat{P}_n}^\pi} \{g(s, a)\} = \gamma \mathbb{E}_{(\tilde{s}, \tilde{a}) \sim d_{\widehat{P}_n}^\pi, s \sim \widehat{P}_n(\cdot | \tilde{s}, \tilde{a}), a \sim \pi(\cdot | s)} \{g(s, a)\} + (1 - \gamma) \mathbb{E}_{s \sim \rho, a \sim \pi(\cdot | s)} \{g(s, a)\}.$$

For the second term, note that $d_{\widehat{P}}^\pi(s) \geq (1 - \gamma) \rho(s)$, hence

$$\begin{aligned}&(1 - \gamma) \mathbb{E}_{s \sim \rho, a \sim \pi(\cdot | s)} \{g(s, a)\} \\ &\leq (1 - \gamma) \sqrt{\mathbb{E}_{s \sim \rho, a \sim \pi(\cdot | s)} \{g^2(s, a)\}} \\ &= (1 - \gamma) \sqrt{\mathbb{E}_{s \sim \rho_n, a \sim \mathcal{U}(\mathcal{A})} \left\{ \frac{\rho(s) \pi(a | s) |\mathcal{A}|}{\rho_n(s)} g^2(s, a) \right\}} \\ &\leq \sqrt{(1 - \gamma) |\mathcal{A}| \mathbb{E}_{s \sim \rho_n, a \sim \mathcal{U}(\mathcal{A})} \{g^2(s, a)\}}.\end{aligned}$$

For the first term, we have that

$$\begin{aligned}&\mathbb{E}_{(\tilde{s}, \tilde{a}) \sim d_{\widehat{P}_n}^\pi, s \sim \widehat{P}_n(\cdot | \tilde{s}, \tilde{a}), a \sim \pi(\cdot | s)} \{g(s, a)\} \\ &= \mathbb{E}_{(\tilde{s}, \tilde{a}) \sim d_{\widehat{P}_n}^\pi} \widehat{\phi}_n(\tilde{s}, \tilde{a})^\top \left[\int_{\mathcal{S} \times \mathcal{A}} \widehat{\mu}_n(s) \pi(a | s) g(s, a) ds da \right] \\ &\leq \mathbb{E}_{(\tilde{s}, \tilde{a}) \sim d_{\widehat{P}_n}^\pi} \left\| \widehat{\phi}_n(\tilde{s}, \tilde{a}) \right\|_{\Sigma_{\rho_n \times \mathcal{U}, \widehat{\phi}_n}^{-1}} \left\| \int_{\mathcal{S} \times \mathcal{A}} \widehat{\mu}_n(s) \pi(a | s) g(s, a) ds da \right\|_{\Sigma_{\rho_n \times \mathcal{U}, \widehat{\phi}_n}},\end{aligned}$$

where for the inequality we use the generalized Cauchy-Schwartz inequality. Note

$$\begin{aligned}&\left\| \int_{\mathcal{S} \times \mathcal{A}} \widehat{\mu}_n(s) \pi(a | s) g(s, a) ds da \right\|_{\Sigma_{\rho_n \times \mathcal{U}, \widehat{\phi}_n}}^2 \\ &= n \mathbb{E}_{\tilde{s} \sim \rho_n, \tilde{a} \sim \mathcal{U}(\mathcal{A})} \left[\left(\int_{\mathcal{S} \times \mathcal{A}} \widehat{P}_n(s | \tilde{s}, \tilde{a}) \pi(a | s) g(s, a) ds da \right)^2 \right] + \lambda_n \left\| \int_{\mathcal{S} \times \mathcal{A}} \widehat{\mu}_n(s) \pi(a | s) g(s, a) ds da \right\|^2 \\ &\leq 2n \mathbb{E}_{\tilde{s} \sim \rho_n, \tilde{a} \sim \mathcal{U}(\mathcal{A})} \left[\left(\int_{\mathcal{S} \times \mathcal{A}} P(s | \tilde{s}, \tilde{a}) \pi(a | s) g(s, a) ds da \right)^2 \right] \\ &\quad + 2n \mathbb{E}_{\tilde{s} \sim \rho_n, \tilde{a} \sim \mathcal{U}(\mathcal{A})} \left[\left(\int_{\mathcal{S} \times \mathcal{A}} (\widehat{P}_n(s | \tilde{s}, \tilde{a}) - P(s | \tilde{s}, \tilde{a})) \pi(a | s) g(s, a) ds da \right)^2 \right] + \lambda_n B_\infty^2 d.\end{aligned}$$

With Jensen's inequality, we have

$$\begin{aligned}&\mathbb{E}_{\tilde{s} \sim \rho_n, \tilde{a} \sim \mathcal{U}(\mathcal{A})} \left[\left(\int_{\mathcal{S} \times \mathcal{A}} P(s | \tilde{s}, \tilde{a}) \pi(a | s) g(s, a) ds da \right)^2 \right] \\ &\leq \mathbb{E}_{\tilde{s} \sim \rho_n, \tilde{a} \sim \mathcal{U}(\mathcal{A}), s \sim P(\cdot | \tilde{s}, \tilde{a}), a \sim \pi(\cdot | s)} \{g^2(s, a)\} \\ &= \mathbb{E}_{s \sim \rho'_n, a \sim \pi(\cdot | s)} \{g^2(s, a)\}\end{aligned}$$

$$\leq |\mathcal{A}| \mathbb{E}_{s \sim \rho'_n, a \sim \mathcal{U}(\mathcal{A})} \{g^2(s, a)\}$$

Meanwhile,

$$\begin{aligned} & \mathbb{E}_{\tilde{s} \sim \rho_n, \tilde{a} \sim \mathcal{U}(\mathcal{A})} \left[\left(\int_{\mathcal{S} \times \mathcal{A}} (\hat{P}_n(s|\tilde{s}, \tilde{a}) - P(s|\tilde{s}, \tilde{a})) \pi(a|s) g(s, a) \, ds \, da \right)^2 \right] \\ & \leq \mathbb{E}_{\tilde{s} \sim \rho_n, \tilde{a} \sim \mathcal{U}(\mathcal{A})} \left[\left\| \hat{P}_n(\cdot|\tilde{s}, \tilde{a}) - P(\cdot|\tilde{s}, \tilde{a}) \right\|_2^2 \left\| \int_{\mathcal{A}} \pi(a|\cdot) g(\cdot, a) \, da \right\|_2^2 \right] \\ & \leq \mathbb{E}_{\tilde{s} \sim \rho_n, \tilde{a} \sim \mathcal{U}(\mathcal{A})} \left[\left\| \hat{P}_n(\cdot|\tilde{s}, \tilde{a}) - P(\cdot|\tilde{s}, \tilde{a}) \right\|_2^2 \left\| \int_{\mathcal{A}} g(\cdot, a) \, da \right\|_2^2 \right] \\ & \leq B_2^2 \zeta_n, \end{aligned}$$

where the last inequality is due to Theorem 5. Substitute back, we obtain the desired result. \square

Lemma 8 (Concentration of the bonus term). *Let $\lambda_n = \Theta(d \log(n|\mathcal{F}|/\delta))$, and define:*

$$\begin{aligned} \Sigma_{\rho_n \times \mathcal{U}, \phi} &= n \mathbb{E}_{s \sim \rho_n, a \sim \mathcal{U}(\mathcal{A})} \phi(s, a) \phi(s, a)^\top + \lambda_n I, \\ \hat{\Sigma}_{n, \phi} &= \sum_{i \in [n]} \phi(s_i, a_i) \phi(s_i, a_i)^\top + \lambda_n I. \end{aligned}$$

Then there exists absolute constant c_1 and c_2 , such that

$$\forall n \in \mathbb{N}^+, \forall \phi \in \Phi, c_1 \|\phi(s, a)\|_{\Sigma_{\rho_n \times \mathcal{U}, \phi}^{-1}} \leq \|\phi(s, a)\|_{\hat{\Sigma}_{n, \phi}^{-1}} \leq c_2 \|\phi(s, a)\|_{\Sigma_{\rho_n \times \mathcal{U}, \phi}^{-1}}$$

which holds with probability at least $1 - \delta$.

Proof. See [Uehara et al., 2021, Lemma 11]. \square

With these lemmas, we are now ready to show the optimism.

Lemma 9 (Optimism). *Let*

$$\begin{aligned} \alpha_n &= \Theta \left(\frac{d \sqrt{|\mathcal{A}| n \zeta_n}}{1 - \gamma} \right), \\ \lambda_n &= \Theta(d \log(n|\mathcal{F}|/\delta)), \end{aligned}$$

then for any policy π we have

$$V_{\hat{P}_n, r+b_n}^\pi \geq V_{P, r}^\pi - \sqrt{\frac{2|\mathcal{A}|d \left(1 + \frac{\gamma^2 d}{(1-\gamma)^2}\right) \zeta_n}{(1-\gamma)}}.$$

Proof. With the simulation lemma (i.e., Lemma 19), we have that

$$\begin{aligned} & V_{\hat{P}_n, r+b_n}^\pi - V_{P, r}^\pi \\ &= \frac{1}{1-\gamma} \mathbb{E}_{(s, a) \sim d_{\hat{P}_n}^\pi} \left[b_n(s, a) + \gamma \mathbb{E}_{\hat{P}_n(s'|s, a)} [V_{P, r}^\pi(s')] - \gamma \mathbb{E}_{P(s'|s, a)} [V_{P, r}^\pi(s')] \right]. \end{aligned}$$

Consider the function g on $\mathcal{S} \times \mathcal{A}$ defined as follows:

$$g(s, a) := \left| \mathbb{E}_{P(s'|s, a)} [V_{P, r}^\pi(s')] - \mathbb{E}_{\hat{P}_n(s'|s, a)} [V_{P, r}^\pi(s')] \right|.$$

With Hölder's inequality, we have that $\|g\|_\infty \leq \frac{2}{1-\gamma}$. Furthermore, as

$$\begin{aligned} g(s, a) &\leq \phi^*(s, a)^\top \int_{\mathcal{S}} \mu^*(s') V_{P, r}^\pi(s') \, ds' + \hat{\phi}_n(s, a)^\top \int_{\mathcal{S}} \hat{\mu}_n^\top(s') V_{P, r, h+1}^\pi(s') \, ds' \\ &\leq \|\phi^*(s, a)\| \left\| \int_{\mathcal{S}} \mu^*(s') V_{P, r}^\pi(s') \, ds' \right\| + \|\hat{\phi}_n(s, a)\| \left\| \int_{\mathcal{S}} \hat{\mu}_n^\top(s') V_{P, r}^\pi(s') \, ds' \right\| \\ &\leq \frac{\sqrt{d}}{1-\gamma} \left(\|\phi^*(s, a)\| + \|\hat{\phi}_n(s, a)\| \right) \end{aligned}$$

where the first inequality is due to the triangle inequality; the second inequality is from the Cauchy-Schwartz inequality; and the last inequality comes from the fact that $\|V_{P, r}^\pi\|_\infty \leq \frac{1}{1-\gamma}$. Thus, we

have

$$\begin{aligned}
\left\| \int_{\mathcal{A}} g(\cdot, a) \, da \right\|_2^2 &= \int_{\mathcal{S}} \left(\int_{\mathcal{A}} g(s, a) \, da \right)^2 \, ds \\
&\leq \frac{d}{(1-\gamma)^2} \int_{\mathcal{S}} \left(\int_{\mathcal{A}} \|\phi^*(s, a)\| \, da + \int_{\mathcal{A}} \|\widehat{\phi}_n(s, a)\| \, da \right)^2 \, ds \\
&\leq \frac{4d^2}{(1-\gamma)^2},
\end{aligned}$$

where the last inequality is due to Assumption 2 and the fact that $(a+b)^2 \leq 2(a^2+b^2)$. Invoking Lemma 7, we have that

$$\begin{aligned}
\mathbb{E}_{(s,a) \sim d_{\widehat{P}_n}^\pi} \{g(s, a)\} &\leq \sqrt{(1-\gamma)|\mathcal{A}| \mathbb{E}_{s \sim \rho_n, a \sim \mathcal{U}(\mathcal{A})} \{g^2(s, a)\}} \\
&+ \gamma \sqrt{n|\mathcal{A}| \mathbb{E}_{s \sim \rho'_n, a \sim \mathcal{U}(\mathcal{A})} \{g^2(s, a)\} + \frac{4d^2}{(1-\gamma)^2} n\zeta_n + \frac{4\lambda_n d}{(1-\gamma)^2} \cdot \mathbb{E}_{(\tilde{s}, \tilde{a}) \sim d_{\widehat{P}_n}^\pi} \left[\left\| \widehat{\phi}_n(\tilde{s}, \tilde{a}) \right\|_{\Sigma_{\rho_n \times \mathcal{U}, \widehat{\phi}_n}^{-1}} \right]}.
\end{aligned}$$

Note that

$$\begin{aligned}
&\mathbb{E}_{s \sim \rho_n, a \sim \mathcal{U}(\mathcal{A})} \{g^2(s, a)\} \\
&= \mathbb{E}_{s \sim \rho_n, a \sim \mathcal{U}(\mathcal{A})} \left(\int_{\mathcal{S}} \left(P(s'|s, a) - \widehat{P}_n(s'|s, a) \right) V_{P,r}^\pi(s') \, ds' \right)^2 \\
&\leq \mathbb{E}_{s \sim \rho_n, a \sim \mathcal{U}(\mathcal{A})} \left\| P(\cdot|s, a) - \widehat{P}_n(\cdot|s, a) \right\|_2^2 \|V_{P,r}^\pi\|_2^2 \\
&\leq 2d \left(1 + \frac{d\gamma^2}{(1-\gamma)^2} \right) \zeta_n,
\end{aligned}$$

where the first inequality is due to the Hölder's inequality and the last inequality is due to Lemma 6. With the selected hyperparameters and Lemma 8, we conclude the proof. \square

To further provide the regret bound, we need the following analog of Lemma 7. Note that, here we don't require ρ'_n .

Lemma 10 (One-step back inequality for the true model). *Assume $g : \mathcal{S} \times \mathcal{A} \rightarrow \mathbb{R}$ satisfies that $\|g\|_\infty \leq B_\infty$, then we have that*

$$\begin{aligned}
\left| \mathbb{E}_{(s,a) \sim d_{P^n}^\pi} \{g(s, a)\} \right| &\leq \sqrt{(1-\gamma)|\mathcal{A}| \mathbb{E}_{s \sim \rho_n, a \sim \mathcal{U}(\mathcal{A})} \{g^2(s, a)\}} \\
&+ \sqrt{n\gamma|\mathcal{A}| \mathbb{E}_{s \sim \rho_n, a \sim \mathcal{U}(\mathcal{A})} \{g^2(s, a)\} + \lambda_n \gamma^2 B_\infty^2 d \cdot \mathbb{E}_{(\tilde{s}, \tilde{a}) \sim d_{P^n}^\pi} \left[\|\phi^*(\tilde{s}, \tilde{a})\|_{\Sigma_{\rho_n, \phi^*}^{-1}} \right]}.
\end{aligned}$$

Proof. Note that

$$\begin{aligned}
&\mathbb{E}_{(s,a) \sim d_{P^n}^\pi} \{g(s, a)\} \\
&= \gamma \mathbb{E}_{(\tilde{s}, \tilde{a}) \sim d_{P^n}^\pi, s \sim P(\cdot|\tilde{s}, \tilde{a}), a \sim \pi(\cdot|s)} \{g(s, a)\} + (1-\gamma) \mathbb{E}_{s \sim \rho, a \sim \pi(\cdot|s)} \{g(s, a)\}.
\end{aligned}$$

For the second term, note that $d_{P^n}^\pi(s) \geq (1-\gamma)\rho(s)$, hence

$$\begin{aligned}
&(1-\gamma) \mathbb{E}_{s \sim \rho, a \sim \pi(\cdot|s)} \{g(s, a)\} \\
&\leq (1-\gamma) \sqrt{\mathbb{E}_{s \sim \rho, a \sim \pi(\cdot|s)} \{g^2(s, a)\}} \\
&= (1-\gamma) \sqrt{\mathbb{E}_{s \sim \rho_n, a \sim \mathcal{U}(\mathcal{A})} \left\{ \frac{\rho(s)\pi(a|s)|\mathcal{A}|}{\rho_n(s)} g^2(s, a) \right\}} \\
&\leq \sqrt{(1-\gamma)|\mathcal{A}| \mathbb{E}_{s \sim \rho_n, a \sim \mathcal{U}(\mathcal{A})} \{g^2(s, a)\}}.
\end{aligned}$$

For the first term, we have that

$$\begin{aligned}
&\mathbb{E}_{(\tilde{s}, \tilde{a}) \sim d_{P^n}^\pi, s \sim P(\cdot|\tilde{s}, \tilde{a}), a \sim \pi(\cdot|s)} \{g(s, a)\} \\
&= \mathbb{E}_{(\tilde{s}, \tilde{a}) \sim d_{P^n}^\pi} \phi^*(\tilde{s}, \tilde{a})^\top \left[\int_{\mathcal{S} \times \mathcal{A}} \mu^*(s) \pi(a|s) g(s, a) \, ds \, da \right] \\
&\leq \mathbb{E}_{(\tilde{s}, \tilde{a}) \sim d_{P^n}^\pi} \|\phi^*(\tilde{s}, \tilde{a})\|_{\Sigma_{\rho_n, \phi^*}^{-1}} \left\| \int_{\mathcal{S} \times \mathcal{A}} \mu^*(s) \pi(a|s) g(s, a) \, ds \, da \right\|_{\Sigma_{\rho_n, \phi^*}},
\end{aligned}$$

where for the inequality we use the generalized Cauchy-Schwartz inequality. Note

$$\begin{aligned}
& \left\| \int_{\mathcal{S} \times \mathcal{A}} \mu^*(s) \pi(a|s) g(s, a) \, ds \, da \right\|_{\Sigma_{\rho_n, \phi^*}}^2 \\
&= n \mathbb{E}_{(\tilde{s}, \tilde{a}) \sim \rho_n} \left[\left(\int_{\mathcal{S} \times \mathcal{A}} P(s|\tilde{s}, \tilde{a}) \pi(a|s) g(s, a) \, ds \, da \right)^2 \right] + \lambda_n \left\| \int_{\mathcal{S} \times \mathcal{A}} \mu^*(s) \pi(a|s) g(s, a) \, ds \, da \right\|^2 \\
&\leq n \mathbb{E}_{(\tilde{s}, \tilde{a}) \sim \rho_n, s \sim P(\cdot|s, a), a \sim \pi(\cdot|s)} \{g^2(s, a)\} + \lambda_n B_\infty^2 d,
\end{aligned}$$

where in the last inequality we use Jensen's inequality. Note that

$$\begin{aligned}
& \mathbb{E}_{(\tilde{s}, \tilde{a}) \sim \rho_n, s \sim P(\cdot|s, a), a \sim \pi(\cdot|s)} \{g^2(s, a)\} \\
&\leq \frac{1}{\gamma} \mathbb{E}_{(\tilde{s}, \tilde{a}) \sim \rho_n, s \sim P^*(\cdot|s, a), a \sim \pi(\cdot|s)} \{g^2(s, a)\} \\
&\leq \frac{|\mathcal{A}|}{\gamma} \mathbb{E}_{s \sim \rho_n, a \sim \mathcal{U}(\mathcal{A})} \{g^2(s, a)\}
\end{aligned}$$

Substituting this back, we obtain the desired result. \square

We also need the following properties on the bonus and the value function when we plan on the learned model with the bonus.

Lemma 11 (Norm of the Bonus). *We have that*

$$\|b_n(s, a)\|_\infty \leq \frac{\alpha_n}{\sqrt{\lambda_n}} \lesssim \frac{\sqrt{d|\mathcal{A}|}}{1-\gamma}, \quad \left\| \int_{\mathcal{A}} b_n(\cdot, a) \, da \right\| \leq \frac{\alpha_n \sqrt{d}}{\sqrt{\lambda_n}} \lesssim \frac{d\sqrt{|\mathcal{A}|}}{1-\gamma}.$$

Proof. Note that, $\hat{\Sigma}_{n, \hat{\phi}_n} \succeq \lambda_n I$, and as a result, we have $\|\hat{\Sigma}_{n, \hat{\phi}_n}^{-1}\|_{\text{op}} \leq \frac{1}{\lambda_n}$. Recall $b_n(s, a) = \alpha_n \|\hat{\phi}_n(s, a)\|_{\hat{\Sigma}_{n, \hat{\phi}_n}^{-1}}$, we know

$$b_n^2(s, a) = \alpha_n^2 \hat{\phi}_n(s, a) \hat{\Sigma}_{n, \hat{\phi}_n}^{-1} \hat{\phi}_n(s, a) \leq \frac{\alpha_n^2 \|\hat{\phi}_n(s, a)\|_2^2}{\lambda_n} \leq \frac{\alpha_n^2}{\lambda_n},$$

as well as

$$\begin{aligned}
& \left\| \int_{\mathcal{A}} b_n(\cdot, a) \, da \right\|^2 \\
&= \alpha_n^2 \left\| \int_{\mathcal{A}} \|\hat{\phi}_n(\cdot, a)\|_{\hat{\Sigma}_{n, \hat{\phi}_n}^{-1}} \, da \right\|^2 \\
&= \alpha_n^2 \int_{\mathcal{S}} \left(\int_{\mathcal{A}} \|\hat{\phi}_n(\cdot, a)\|_{\hat{\Sigma}_{n, \hat{\phi}_n}^{-1}} \, da \right)^2 \, ds \\
&\leq \frac{\alpha_n^2}{\lambda_n} \int_{\mathcal{S}} \left(\int_{\mathcal{A}} \|\hat{\phi}_n(s, a)\| \, da \right)^2 \, ds \\
&\leq \frac{\alpha_n^2 d}{\lambda_n},
\end{aligned}$$

Combined with the fact that $\frac{\alpha_n}{\sqrt{\lambda_n}} = \Theta\left(\frac{\sqrt{d|\mathcal{A}|}}{1-\gamma}\right)$, we conclude the proof. \square

Lemma 12 (L_2 norm of $V_{\hat{P}_n, r+b_n}^\pi$). *For any policy π , we have that*

$$\|V_{\hat{P}_n, r+b_n}^\pi\| \leq \sqrt{3d + \frac{3\alpha_n^2 d}{\lambda_n} + \frac{3d^2 \gamma^2 \left(1 + \frac{\alpha_n}{\sqrt{\lambda_n}}\right)^2}{(1-\gamma)^2}} \lesssim \frac{d^{1.5} \sqrt{|\mathcal{A}|}}{(1-\gamma)^2}$$

Proof. We have

$$\begin{aligned}
& \|V_{\hat{P}_n, r+b_n}^\pi\|^2 \\
&= \int_{\mathcal{S}} \left(V_{\hat{P}_n, r+b_n}^\pi(s) \right)^2 \, ds
\end{aligned}$$

$$\begin{aligned}
&= \int_S \left(\int_{\mathcal{A}} \pi(a|s) \left(r(s, a) + b_n(s, a) + \gamma Q_{\hat{P}_n, r+b_n}^\pi(s, a) \right) da \right)^2 ds \\
&\leq \int_S \left(\int_{\mathcal{A}} \left(r(s, a) + b_n(s, a) + \gamma Q_{\hat{P}_n, r+b_n}^\pi(s, a) \right) da \right)^2 ds \\
&\leq 3 \int_S \left(\int_{\mathcal{A}} [r(s, a)]^2 da \right) ds + 3 \int_S \left(\int_{\mathcal{A}} \left[\alpha_n \left\| \hat{\phi}_n(s, a) \right\|_{\Sigma_{\rho_n, \hat{\phi}_n}^{-1}} da \right]^2 da \right) ds \\
&\quad + 3\gamma^2 \int_S \left(\int_{\mathcal{A}} \left[Q_{\hat{P}_n, r+b_n}^\pi(s, a) \right]^2 da \right)^2 ds \\
&\leq 3d + \frac{3\alpha_n^2 d}{\lambda_n} + \frac{3d^2 \gamma^2 \left(1 + \frac{\alpha_n}{\sqrt{\lambda_n}} \right)^2}{(1-\gamma)^2} \\
&\lesssim \frac{d^3 |\mathcal{A}|}{(1-\gamma)^4},
\end{aligned}$$

which concludes the proof. \square

Now we are ready to prove the following regret bounds and obtain the final PAC guarantee.

Lemma 13 (Regret). *With probability at least $1 - \delta$, we have that*

$$\sum_{n=1}^N V_{P,r}^* - V_{P,r}^{\pi_n} \lesssim \sqrt{\frac{Nd^4 |\mathcal{A}|^2 \log(N|\mathcal{F}|/\delta)}{(1-\gamma)^6}} \log \left(1 + \frac{N}{d^2 \log(N|\mathcal{F}|/\delta)} \right).$$

Proof. Standard decomposition shows

$$\begin{aligned}
&V_{P,r}^* - V_{P,r}^{\pi_n} \\
&\leq V_{\hat{P}_n, r+b_n}^* + \sqrt{\frac{2|\mathcal{A}|d \left(1 + \frac{\gamma^2 d}{(1-\gamma)^2} \right) \zeta_n}{(1-\gamma)}} - V_{P,r}^{\pi_n} \\
&\leq V_{\hat{P}_n, r+b_n}^{\pi_n} - V_{P,r}^{\pi_n} + \sqrt{\frac{2|\mathcal{A}|d \left(1 + \frac{\gamma^2 d}{(1-\gamma)^2} \right) \zeta_n}{(1-\gamma)}} \\
&\leq \frac{1}{1-\gamma} \mathbb{E}_{(s,a) \sim d_P^{\pi_n}} \left[b_n(s, a) + \gamma \mathbb{E}_{\hat{P}_n(s'|s,a)} [V_{\hat{P}_n, r+b_n}^{\pi_n}(s')] - \gamma \mathbb{E}_{P(s'|s,a)} [V_{\hat{P}_n, r+b_n}^{\pi_n}(s')] \right] \\
&\quad + \sqrt{\frac{2|\mathcal{A}|d \left(1 + \frac{\gamma^2 d}{(1-\gamma)^2} \right) \zeta_n}{(1-\gamma)}}.
\end{aligned}$$

Applying Lemma 10 to $\mathbb{E}_{(s,a) \sim d_P^{\pi_n}} \{b_n(s, a)\}$, we have that

$$\begin{aligned}
&\mathbb{E}_{(s,a) \sim d_P^{\pi_n}} \{b_n(s, a)\} \\
&\leq \sqrt{(1-\gamma) |\mathcal{A}| \mathbb{E}_{s \sim \rho_n, a \sim \mathcal{U}(\mathcal{A})} \{b_n^2(s, a)\}} \\
&\quad + \sqrt{n\gamma |\mathcal{A}| \mathbb{E}_{s \sim \rho_n, a \sim \mathcal{U}(\mathcal{A})} \{b_n^2(s, a)\} + \gamma^2 \alpha_n^2 d \mathbb{E}_{(\tilde{s}, \tilde{a}) \sim d_P^{\pi_n}} \left[\left\| \phi^*(\tilde{s}, \tilde{a}) \right\|_{\Sigma_{\rho_n, \phi^*}^{-1}} \right]}.
\end{aligned}$$

Note that

$$\begin{aligned}
&\mathbb{E}_{s \sim \rho_n, a \sim \mathcal{U}(\mathcal{A})} \left\| \hat{\phi}_n(s, a) \right\|_{\Sigma_{\rho_n, \hat{\phi}_n}^{-1}}^2 \\
&= \mathbb{E}_{s \sim \rho_n, a \sim \mathcal{U}(\mathcal{A})} \left[\hat{\phi}_n(s, a)^\top \Sigma_{\rho_n, \hat{\phi}_n}^{-1} \hat{\phi}_n(s, a) \right] \\
&= \text{Tr} \left(\mathbb{E}_{s \sim \rho_n, a \sim \mathcal{U}(\mathcal{A})} \left[\hat{\phi}_n(s, a) \hat{\phi}_n(s, a)^\top \right] \left(n \mathbb{E}_{s \sim \rho_n, a \sim \mathcal{U}(\mathcal{A})} \left[\hat{\phi}_n(s, a) \hat{\phi}_n(s, a)^\top \right] + \lambda_n I \right)^{-1} \right) \\
&\leq \frac{d}{n},
\end{aligned}$$

hence, with the concentration of the bonus, we have

$$\mathbb{E}_{(s,a) \sim d_P^{\pi_n}} \{b_n(s, a)\} \lesssim \sqrt{\frac{(1-\gamma)\alpha_n^2 d|\mathcal{A}|}{n}} + \sqrt{\gamma\alpha_n^2 d|\mathcal{A}| + \gamma^2\alpha_n^2 d} \cdot \mathbb{E}_{(\tilde{s}, \tilde{a}) \sim d_P^{\pi_n}} \left[\|\phi^*(\tilde{s}, \tilde{a})\|_{\Sigma_{\rho_n, \phi^*}^{-1}} \right].$$

We then consider the remaining term. With a slightly abuse of notation, define $g(s, a) :=$

$$\left| \mathbb{E}_{\hat{P}_n(s'|s, a)} V_{\hat{P}_n, r+b_n}^{\pi_n}(s') - \mathbb{E}_{P(s'|s, a)} V_{\hat{P}_n, r+b_n}^{\pi_n}(s') \right|. \quad \text{With Hölder's inequality, we know that}$$

$$\|g(s, a)\|_\infty \leq 2 \left\| V_{\hat{P}_n, r+b_n}^{\pi_n} \right\|_\infty \leq \frac{2 \left(1 + \frac{\alpha_n}{\sqrt{\lambda_n}}\right)}{1-\gamma} \lesssim \frac{\sqrt{d|\mathcal{A}|}}{(1-\gamma)^2}. \quad \text{Applying Lemma 10 to } \mathbb{E}_{(s,a) \sim d_P^{\pi_n}} \{g(s, a)\}, \text{ we have that}$$

$$\begin{aligned} & \mathbb{E}_{(s,a) \sim d_P^{\pi_n}} \{g(s, a)\} \\ & \leq \sqrt{(1-\gamma)|\mathcal{A}| \mathbb{E}_{s \sim \rho_n, a \sim \mathcal{U}(\mathcal{A})} \{g^2(s, a)\}} \\ & \quad + \sqrt{n\gamma|\mathcal{A}| \mathbb{E}_{s \sim \rho_n, a \sim \mathcal{U}(\mathcal{A})} \{g^2(s, a)\} + \frac{4\gamma^2 d (\sqrt{\lambda_n} + \alpha_n)^2}{(1-\gamma)^2} \mathbb{E}_{(\tilde{s}, \tilde{a}) \sim d_P^{\pi_n}} \left[\|\phi^*(\tilde{s}, \tilde{a})\|_{\Sigma_{\rho_n, \phi^*}^{-1}} \right]}. \end{aligned}$$

Note that

$$\begin{aligned} & \mathbb{E}_{s \sim \rho_n, a \sim \mathcal{U}(\mathcal{A})} \{g^2(s, a)\} \\ & = \mathbb{E}_{s \sim \rho_n, a \sim \mathcal{U}(\mathcal{A})} \left[\left(\int_{\mathcal{S}} \left(\hat{P}_n(s'|s, a) - P(s'|s, a) \right) V_{\hat{P}_n, r+b_n}^{\pi_n}(s') \right)^2 \right] \\ & \leq \mathbb{E}_{s \sim \rho_n, a \sim \mathcal{U}(\mathcal{A})} \left[\left\| \hat{P}_n(\cdot|s, a) - P(\cdot|s, a) \right\|^2 \left\| V_{\hat{P}_n, r+b_n}^{\pi_n} \right\|^2 \right] \\ & \leq 3d \left(1 + \frac{\alpha_n^2}{\lambda_n} + \frac{d\gamma^2 \left(1 + \frac{\alpha_n}{\sqrt{\lambda_n}}\right)^2}{(1-\gamma)^2} \right) \zeta_n \lesssim \frac{d^3 |\mathcal{A}| \zeta_n}{(1-\gamma)^4} \end{aligned}$$

Hence,

$$\begin{aligned} & \mathbb{E}_{(s,a) \sim d_P^{\pi_n}} \{g(s, a)\} \lesssim \sqrt{(1-\gamma)d^3 |\mathcal{A}|^2 \zeta_n} \\ & \quad + \sqrt{\frac{d^3 |\mathcal{A}|^2 n \zeta_n}{(1-\gamma)^4} + \frac{d^3 |\mathcal{A}| n \zeta_n}{(1-\gamma)^4} \mathbb{E}_{(\tilde{s}, \tilde{a}) \sim d_P^{\pi_n}} \left[\|\phi^*(\tilde{s}, \tilde{a})\|_{\Sigma_{\rho_n, \phi^*}^{-1}} \right]}. \end{aligned}$$

Finally, with Lemma 20 and notice that $\lambda_1 \leq \lambda_2 \leq \dots \leq \lambda_n$, we have that

$$\begin{aligned} & \sum_{n=1}^N \mathbb{E}_{(\tilde{s}, \tilde{a}) \sim d_P^{\pi_n}} \left[\|\phi^*(\tilde{s}, \tilde{a})\|_{\Sigma_{\rho_n, \phi^*}^{-1}} \right] \\ & \leq \sqrt{N \text{Tr} \left(\left(\mathbb{E}_{(\tilde{s}, \tilde{a}) \sim d_P^{\pi_n}} \phi^*(\tilde{s}, \tilde{a}) (\phi^*(\tilde{s}, \tilde{a}))^\top \right) \Sigma_{\rho_n, \phi^*}^{-1} \right)} \\ & \leq \sqrt{Nd \log \frac{\lambda_N + N}{\lambda_1}} \end{aligned}$$

Combine the previous terms and take the dominating terms out, we have that

$$\sum_{n=1}^N V_{P, r}^{\pi_n^*} - V_{P, r}^{\pi_n} \lesssim \sqrt{\frac{Nd^4 |\mathcal{A}|^2 \log(N|\mathcal{F}|/\delta)}{(1-\gamma)^6} \log \left(1 + \frac{N}{d^2 \log(N|\mathcal{F}|/\delta)} \right)},$$

which concludes the proof. \square

Theorem 14 (PAC Guarantee). *After interacting with the environments for $N = \tilde{\Theta} \left(\frac{d^4 |\mathcal{A}|^2}{(1-\gamma)^6 \epsilon^2} \right)$ episodes, we can obtain an ϵ -optimal policy with high probability. Furthermore, with high probability, for each episode, we can terminate within $\tilde{\Theta}(1/(1-\gamma))$ steps.*

Proof. It directly follows from the standard regret to PAC reduction. See Jin et al. [2018], Uehara et al. [2021] for the detail. \square

C.3 PAC bounds for Offline Reinforcement Learning

Proof Sketch Similar to the online counterpart, our proof for offline setting is organized as follows:

- We show the policy obtained by planning on the learned model with additional penalty lower bound the optimal value up to some error term (Lemma 16), with the help of an analog of the one-step back inequality for the learned model in the offline setting (Lemma 15) based on Theorem 5.
- We then show the PAC guarantee (Theorem 18) with an analog of the one-step back inequality for the true model in the offline setting (Lemma 17).

We first prove the analog of Lemma 7 in the offline setting.

Lemma 15 (One-step back inequality for the learned model in the offline setting). *Let $\omega = \max_{s,a} \{1/\pi_b(a|s)\}$. Assume $g : \mathcal{S} \times \mathcal{A} \rightarrow \mathbb{R}$ satisfies that $\|g\|_\infty \leq B_\infty$, $\|\int_{\mathcal{A}} g(\cdot, a) da\|_2 \leq B_2$, then we have that*

$$\begin{aligned} \left| \mathbb{E}_{(s,a) \sim d_{\hat{P}}^\pi} \{g(s, a)\} \right| &\leq \sqrt{(1-\gamma)\omega \mathbb{E}_{(s,a) \sim \rho_b} \{g^2(s, a)\}} \\ &+ \gamma \sqrt{n\omega \mathbb{E}_{(s,a) \sim \rho_b} \{g^2(s, a)\} + B_2^2 n \zeta_n + \lambda_n B_\infty^2 d \cdot \mathbb{E}_{\tilde{s}, \tilde{a} \sim d_{\hat{P}}^\pi} \left[\left\| \hat{\phi}(\tilde{s}, \tilde{a}) \right\|_{\Sigma_{\rho_b, \hat{\phi}}^{-1}}^2 \right]}. \end{aligned}$$

Proof. Note that

$$\mathbb{E}_{(s,a) \sim d_{\hat{P}}^\pi} \{g(s, a)\} = \gamma \mathbb{E}_{(\tilde{s}, \tilde{a}) \sim d_{\hat{P}}^\pi, s \sim \hat{P}(\cdot|\tilde{s}, \tilde{a}), a \sim \pi(\cdot|s)} \{g(s, a)\} + (1-\gamma) \mathbb{E}_{s \sim \rho, a \sim \pi(\cdot|s)} \{g(s, a)\}.$$

For the second term, we have that

$$\begin{aligned} &(1-\gamma) \mathbb{E}_{s \sim \rho, a \sim \pi(\cdot|s)} \{g(s, a)\} \\ &\leq (1-\gamma) \sqrt{\mathbb{E}_{s \sim \rho, a \sim \pi(\cdot|s)} \{g^2(s, a)\}} \\ &= (1-\gamma) \sqrt{\mathbb{E}_{s \sim \rho_b, a \sim \pi_b(\cdot|s)} \left\{ \frac{\rho(s)\pi(a|s)}{\rho_b(s)\pi(a|s)} g^2(s, a) \right\}} \\ &\leq \sqrt{\omega(1-\gamma) |\mathcal{A}| \mathbb{E}_{s \sim \rho_b, a \sim \pi_b(\cdot|s)} g^2(s, a)}. \end{aligned}$$

For the first term, we have that

$$\begin{aligned} &\mathbb{E}_{(\tilde{s}, \tilde{a}) \sim d_{\hat{P}}^\pi, s \sim \hat{P}(\cdot|\tilde{s}, \tilde{a}), a \sim \pi(\cdot|s)} \{g(s, a)\} \\ &= \mathbb{E}_{(\tilde{s}, \tilde{a}) \sim d_{\hat{P}}^\pi} \hat{\phi}(\tilde{s}, \tilde{a})^\top \left[\int_{\mathcal{S} \times \mathcal{A}} \hat{\mu}(s) \pi(a|s) g(s, a) ds da \right] \\ &\leq \mathbb{E}_{(\tilde{s}, \tilde{a}) \sim d_{\hat{P}}^\pi} \left\| \hat{\phi}(\tilde{s}, \tilde{a}) \right\|_{\Sigma_{\rho_b, \hat{\phi}}^{-1}} \left\| \int_{\mathcal{S} \times \mathcal{A}} \hat{\mu}(s) \pi(a|s) g(s, a) ds da \right\|_{\Sigma_{\rho_b, \hat{\phi}}}. \end{aligned}$$

Note that

$$\begin{aligned} &\left\| \int_{\mathcal{S} \times \mathcal{A}} \hat{\mu}(s) \pi(a|s) g(s, a) ds da \right\|_{\Sigma_{\rho_b, \hat{\phi}}}^2 \\ &= n \mathbb{E}_{(\tilde{s}, \tilde{a}) \sim \rho_b} \left[\left(\int_{\mathcal{S} \times \mathcal{A}} \hat{P}_n(s|\tilde{s}, \tilde{a}) \pi(a|s) g(s, a) ds da \right)^2 \right] + \lambda \left\| \int_{\mathcal{S} \times \mathcal{A}} \hat{\mu}(s) \pi(a|s) g(s, a) \right\|^2 \\ &\leq 2n \mathbb{E}_{(\tilde{s}, \tilde{a}) \sim \rho_b} \left[\left(\int_{\mathcal{S} \times \mathcal{A}} P(s|\tilde{s}, \tilde{a}) \pi(a|s) g(s, a) ds da \right)^2 \right] \\ &\quad + 2n \mathbb{E}_{(\tilde{s}, \tilde{a}) \sim \rho_b} \left[\left(\int_{\mathcal{S} \times \mathcal{A}} \left(\hat{P}(s|\tilde{s}, \tilde{a}) - P(s|\tilde{s}, \tilde{a}) \right) \pi(a|s) g(s, a) ds da \right)^2 \right] + \lambda B_\infty^2 d. \end{aligned}$$

With Jensen's inequality, we have

$$\begin{aligned} &\mathbb{E}_{(\tilde{s}, \tilde{a}) \sim \rho_b} \left[\left(\int_{\mathcal{S} \times \mathcal{A}} P(s|\tilde{s}, \tilde{a}) \pi(a|s) g(s, a) ds da \right)^2 \right] \\ &\leq \mathbb{E}_{(\tilde{s}, \tilde{a}) \sim \rho_b, s \sim P(\cdot|\tilde{s}, \tilde{a}), a \sim \pi(\cdot|s)} \{g^2(s, a)\} \end{aligned}$$

$$\leq \frac{\omega}{\gamma} \mathbb{E}_{(s,a) \sim \rho_b} \{g^2(s, a)\}.$$

On the other hand,

$$\begin{aligned} & \mathbb{E}_{(\tilde{s}, \tilde{a}) \sim \rho_b} \left[\left(\int_{\mathcal{S} \times \mathcal{A}} \left(\hat{P}(s|\tilde{s}, \tilde{a}) - P(s|\tilde{s}, \tilde{a}) \right) \pi(a|s) g(s, a) \, ds \, da \right)^2 \right] \\ & \leq \mathbb{E}_{(\tilde{s}, \tilde{a}) \sim \rho_b} \left[\left\| \hat{P}(\cdot|\tilde{s}, \tilde{a}) - P(\cdot|\tilde{s}, \tilde{a}) \right\|_2^2 \left\| \int_{\mathcal{A}} \pi(a|\cdot) g(\cdot, a) \, da \right\|_2^2 \right] \\ & \leq \mathbb{E}_{(\tilde{s}, \tilde{a}) \sim \rho_b} \left[\left\| \hat{P}(\cdot|\tilde{s}, \tilde{a}) - P(\cdot|\tilde{s}, \tilde{a}) \right\|_2^2 \left\| \int_{\mathcal{A}} g(\cdot, a) \, da \right\|_2^2 \right] \\ & \leq B_2^2 \zeta_n, \end{aligned}$$

where the last inequality is due to Theorem 5. Substituting this back, we obtain the desired result. \square

Lemma 16 (Pessimism). *Let $\omega = \max_{s,a} \{\pi_b(a|s)\}$,*

$$\begin{aligned} \alpha_n &= \Theta \left(\frac{d\sqrt{\omega\zeta_n}}{1-\gamma} \right), \\ \lambda &= \Theta(d \log(|\mathcal{F}|/\delta)), \end{aligned}$$

then we have

$$V_{\hat{P}, r-b}^\pi \leq V_{P, r}^\pi + \sqrt{\frac{2\omega d \left(1 + \frac{\gamma^2 d}{(1-\gamma)^2}\right) \zeta_n}{(1-\gamma)}}.$$

Proof. With the simulation Lemma (i.e., Lemma 19), we have

$$\begin{aligned} & V_{\hat{P}_n, r-b}^\pi - V_{P, r}^\pi \\ &= \frac{1}{1-\gamma} \mathbb{E}_{(s,a) \sim d_{\hat{P}_n}^\pi} \left[-b(s, a) + \gamma \left[\mathbb{E}_{\hat{P}_n(s'|s, a)} [V_{P, r}^\pi(s')] - \mathbb{E}_{P(s'|s, a)} [V_{P, r}^\pi(s')] \right] \right]. \end{aligned}$$

Consider $g(s, a) := \left| \mathbb{E}_{\hat{P}_n(s'|s, a)} [V_{P, r}^\pi(s')] - \mathbb{E}_{P(s'|s, a)} [V_{P, r}^\pi(s')] \right|$. With Hölder's inequality, $\|g\|_\infty \leq \frac{2}{1-\gamma}$. Furthermore, with the derivation in the proof of Lemma 9, we know $\|\int_{\mathcal{A}} g(\cdot, a) \, da\|_2 \leq \frac{\sqrt{2d}}{1-\gamma}$. Applying Lemma 15, we have that

$$\begin{aligned} & \mathbb{E}_{(s,a) \sim d_{\hat{P}}^\pi} \{g(s, a)\} \leq \sqrt{(1-\gamma)\omega \mathbb{E}_{(s,a) \sim \rho_b} \{g^2(s, a)\}} \\ & + \gamma \sqrt{n\omega \mathbb{E}_{(s,a) \sim \rho_b} \{g^2(s, a)\} + \frac{2d^2}{(1-\gamma)^2} \log(|\mathcal{F}|/\delta) + \frac{4\lambda_n d}{(1-\gamma)^2}} \cdot \mathbb{E}_{(\tilde{s}, \tilde{a}) \sim d_{\hat{P}}^\pi} \left[\left\| \hat{\phi}(\tilde{s}, \tilde{a}) \right\|_{\Sigma_{\rho_b, \hat{\phi}}^{-1}} \right]. \end{aligned}$$

With Lemma 6, we know

$$\mathbb{E}_{(s,a) \sim \rho_b} \{g^2(s, a)\} \leq 2d \left(1 + \frac{d\gamma^2}{(1-\gamma)^2}\right) \zeta_n.$$

Then, with the selected hyperparameters and Lemma 8, we conclude the proof. \square

Lemma 17 (One-step back inequality for the true model in the offline setting). *Let $\omega = \max_{s,a} \{\pi_b(a|s)\}$, assume $g : \mathcal{S} \times \mathcal{A} \rightarrow \mathbb{R}$ satisfies $\|g\|_\infty \leq B_\infty$, then we have*

$$\begin{aligned} & \left| \mathbb{E}_{(s,a) \sim d_{\hat{P}}^\pi} \{g(s, a)\} \right| \leq \sqrt{(1-\gamma)\omega \mathbb{E}_{(s,a) \sim \rho_b} \{g^2(s, a)\}} \\ & + \sqrt{n\gamma\omega \mathbb{E}_{(s,a) \sim \rho_b} \{g^2(s, a)\} + \lambda\gamma^2 B_\infty^2 d} \cdot \mathbb{E}_{(\tilde{s}, \tilde{a}) \sim d_{\hat{P}}^\pi} \left[\left\| \phi^*(\tilde{s}, \tilde{a}) \right\|_{\Sigma_{\rho_b, \sigma^*}^{-1}} \right]. \end{aligned}$$

Proof. The proof is identical to the proof of Lemma 7. \square

We now provide the PAC guarantee for the offline setting.

Theorem 18 (PAC Guarantee). *With probability $1 - \delta$, \forall baseline policy π including history-dependent non-Markovian policies, we have that*

$$V_{P,r}^\pi - V_{P,r}^{\hat{\pi}} \lesssim \sqrt{\frac{\omega^2 d^4 C_\pi^* \log(|\mathcal{F}|/\delta)}{(1-\gamma)^6}},$$

where C_π^* is the relative conditional number under ϕ^* , defined as

$$C_\pi^* := \sup_{x \in \mathbb{R}} \frac{x^\top \mathbb{E}_{(s,a) \sim d_P^\pi} [\phi^*(s,a) \phi^*(s,a)^\top] x}{x^\top \mathbb{E}_{(s,a) \sim \rho_b} [\phi^*(s,a) \phi^*(s,a)^\top] x}.$$

Proof. Standard decomposition shows

$$\begin{aligned} & V_{P,r}^\pi - V_{P,r}^{\hat{\pi}} \\ & \leq V_{P,r}^\pi - V_{\hat{P},r-b}^{\hat{\pi}} + \sqrt{\frac{2\omega d \left(1 + \frac{\gamma^2 d}{(1-\gamma^2)}\right) \zeta_n}{(1-\gamma)}} \\ & \leq V_{P,r}^\pi - V_{\hat{P},r-b}^\pi + \sqrt{\frac{2\omega d \left(1 + \frac{\gamma^2 d}{(1-\gamma^2)}\right) \zeta_n}{(1-\gamma)}} \\ & = \mathbb{E}_{(s,a) \sim d_P^\pi} \left[b(s,a) + \gamma \mathbb{E}_{P(s'|s,a)} \left[V_{\hat{P},r-b}^\pi(s') \right] - \gamma \mathbb{E}_{\hat{P}(s'|s,a)} \left[V_{\hat{P},r-b}^\pi(s') \right] \right] \\ & \quad + \sqrt{\frac{2\omega d \left(1 + \frac{\gamma^2 d}{(1-\gamma^2)}\right) \zeta_n}{(1-\gamma)}}. \end{aligned}$$

With Lemma 17 and the identical method used in the proof of Lemma 13, we have that

$$\mathbb{E}_{(s,a) \sim d_P^\pi} \{b_n(s,a)\} \leq \sqrt{\frac{(1-\gamma)\alpha_n^2 d \omega}{n}} + \sqrt{\gamma \alpha_n^2 d \omega + \gamma^2 \alpha_n^2 d} \cdot \mathbb{E}_{(\tilde{s}, \tilde{a}) \sim d_P^\pi} \left[\|\phi^*(\tilde{s}, \tilde{a})\|_{\Sigma_{\rho_b}, \phi^*} \right].$$

Furthermore, define $g(s,a) := \left| \mathbb{E}_{\hat{P}_n(s'|s,a)} V_{\hat{P}_n, r+b_n}^{\pi_n}(s') - \mathbb{E}_{P(s'|s,a)} V_{\hat{P}_n, r+b_n}^{\pi_n}(s') \right|$. With Lemma 17 and the identical method used in the proof of Lemma 13, we can obtain

$$\mathbb{E}_{(s,a) \sim d_P^\pi} \{g(s,a)\} \lesssim \sqrt{(1-\gamma)d^3 \omega^2 \zeta_n} + \sqrt{\frac{d^3 \omega^2 n \zeta_n}{(1-\gamma)^4}} \mathbb{E}_{(\tilde{s}, \tilde{a}) \sim d_P^\pi} \left[\|\phi^*(\tilde{s}, \tilde{a})\|_{\Sigma_{\rho_b}^{-1}, \phi^*} \right].$$

Finally, by the definition of C^* , we have that

$$\begin{aligned} \mathbb{E}_{(\tilde{s}, \tilde{a}) \sim d_P^\pi} \left[\|\phi^*(\tilde{s}, \tilde{a})\|_{\Sigma_{\rho_b, \phi^*}^{-1}} \right] & \leq \sqrt{\mathbb{E}_{(\tilde{s}, \tilde{a}) \sim d_P^\pi} \left[\|\phi^*(\tilde{s}, \tilde{a})\|_{\Sigma_{\rho_b, \phi^*}^{-1}}^2 \right]} \\ & \leq \sqrt{C^* \mathbb{E}_{(\tilde{s}, \tilde{a}) \sim \rho_b} \left[\|\phi^*(\tilde{s}, \tilde{a})\|_{\Sigma_{\rho_b, \phi^*}^{-1}} \right]} \leq \sqrt{\frac{C^* d}{n}}. \end{aligned}$$

Combining the previous terms and taking the dominating terms out, we conclude the proof. \square

D Technical Lemmas

Lemma 19 (Simulation Lemma). *With a slightly abuse of notation, we have*

$$\begin{aligned} V_{\hat{P}_n, r+b}^\pi - V_{P,r}^\pi &= \frac{1}{1-\gamma} \mathbb{E}_{(s,a) \sim d_P^\pi} \left[b(s,a) + \gamma \left[\mathbb{E}_{\hat{P}_n(s'|s,a)} [V_{\hat{P}_n, r+b}^\pi(s')] - \mathbb{E}_{P(s'|s,a)} [V_{\hat{P}_n, r+b}^\pi(s')] \right] \right], \\ V_{\hat{P}_n, r+b}^\pi - V_{P,r}^\pi &= \frac{1}{1-\gamma} \mathbb{E}_{(s,a) \sim d_{\hat{P}_n}^\pi} \left[b(s,a) + \gamma \left[\mathbb{E}_{\hat{P}_n(s'|s,a)} [V_{P,r}^\pi(s')] - \mathbb{E}_{P(s'|s,a)} [V_{P,r}^\pi(s')] \right] \right]. \end{aligned}$$

Proof. Note that

$$\begin{aligned} & \mathbb{E}_{s \sim d_P^\pi, a \sim \pi(\cdot|s)} [f(s,a)] \\ &= (1-\gamma) \mathbb{E}_{s \sim \rho, a \sim \pi(\cdot|s)} [f(s,a)] + \gamma \mathbb{E}_{\tilde{s} \sim d_P^\pi, \tilde{a} \sim \pi(\cdot|\tilde{s}), s \sim P(\cdot|\tilde{s}, \tilde{a}), \tilde{a} \sim \pi(\cdot|\tilde{s})} [f(s,a)]. \end{aligned}$$

Take $f = Q_{\hat{P}_n, r+b}^\pi$, we have that

$$\begin{aligned} V_{\hat{P}_n, r+b}^\pi &= \mathbb{E}_{s \sim \rho, a \sim \pi(\cdot|s)} \left[Q_{\hat{P}_n, r+b}^\pi(s, a) \right] \\ &= \frac{1}{1-\gamma} \left(\mathbb{E}_{s \sim d_P^\pi, a \sim \pi(\cdot|s)} \left[Q_{\hat{P}_n, r+b}^\pi(s, a) \right] - \gamma \mathbb{E}_{\tilde{s} \sim d_P^\pi, \tilde{a} \sim \pi(\cdot|\tilde{s}), s \sim P(\cdot|\tilde{s}, \tilde{a}), \tilde{a} \sim \pi(\cdot|\tilde{s})} \left[Q_{\hat{P}_n, r+b}^\pi(s, a) \right] \right) \\ &= \frac{1}{1-\gamma} \mathbb{E}_{s \sim d_P^\pi, a \sim \pi(\cdot|s)} \left[Q_{\hat{P}_n, r+b}^\pi(s, a) - \gamma \mathbb{E}_{s' \sim P(\cdot|s, a), a' \sim \pi(\cdot|s')} \left[Q_{\hat{P}_n, r+b}^\pi(s', a') \right] \right]. \end{aligned}$$

Substitute back, we have that

$$\begin{aligned} V_{\hat{P}_n, r+b}^\pi - V_{P, r}^\pi &= \frac{1}{1-\gamma} \mathbb{E}_{s \sim d_P^\pi, a \sim \pi(\cdot|s)} \left[Q_{\hat{P}_n, r+b}^\pi(s, a) - \gamma \mathbb{E}_{s' \sim P(\cdot|s, a), a' \sim \pi(\cdot|s')} \left[Q_{\hat{P}_n, r+b}^\pi(s', a') \right] - r(s, a) \right] \\ &= \frac{1}{1-\gamma} \mathbb{E}_{s \sim d_P^\pi, a \sim \pi(\cdot|s)} \left[b(s, a) + \gamma \left[\mathbb{E}_{s' \sim \hat{P}_n(\cdot|s, a)} [V_{\hat{P}_n, r+b}^\pi(s')] - \mathbb{E}_{s' \sim P(\cdot|s, a)} [V_{\hat{P}_n, r+b}^\pi(s')] \right] \right]. \end{aligned}$$

The second equation can be obtained with a similar method, which concludes the proof. \square

Lemma 20 (Elliptical Potential Lemma). *Let $M_0 = \lambda I_{d \times d}$, $M_n = M_{n-1} + G_n$ where G_n is a symmetric positive definite matrix with $\|G_n\|_{op} \leq c$, then we have that*

$$\sum_{n=1}^N \text{Tr}(G_n M_{n-1}^{-1}) \leq \log \det(M_N) - d \log \lambda \leq d \log \left(1 + \frac{Nc}{\lambda} \right).$$

Proof. By the concavity of $\log \det(\cdot)$ function and $\frac{d \log \det(X)}{dX} = (X^\top)^{-1}$, we know

$$\begin{aligned} \log \det(M_n) &\leq \log \det(M_{n-1}) + \text{Tr}(M_{n-1}^{-1}(M_n - M_{n-1})) \\ &= \log \det(M_{n-1}) + \text{Tr}(M_{n-1}^{-1}G_n). \end{aligned}$$

Telescoping, we can obtain the first inequality. For the second inequality, note that, with Jensen's inequality, we have

$$\log \det(M_n) = \sum_{i=1}^d \log \sigma_i \leq d \log \frac{\text{Tr}(M_n)}{d} \leq d \log(\lambda + Nc)$$

where σ_i is the i -th eigenvalue of M_n . \square

E Experiment Details

E.1 Online Setting

We list all the hyperparameter and network architecture we use for our experiments. For online MuJoCo and DM Control tasks, the hyperparameters can be found at Table 4. Therefore, we set bonus scaling term to 0 for MuJoCo tasks. However, this bonus is critical to the success of DM Control Suite (especially sparse reward environments). Note that we use exactly the same actor and critic network architecture for all the algorithms in the DM Control Suite experiment.

For evaluation in Mujoco, in each evaluation (every 5K steps) we test our algorithm for 10 episodes. We average the results over the last 4 evaluations and 4 random seeds. For Dreamer and Proto-RL, we change their network from CNN to 3-layer MLP and disable the image data augmentation part (since we test on the state space). We tried to tune some of their hyperparameter (e.g., exploration steps in Proto-RL) and report the best number across our runs. However, due to the short time, it is also possible that we didn't tune the hyperparameter enough.

E.2 Performance Curves

We provide the performance curves for online DM Control Suite experiments in Figure 4. As we can see in the figures, the proposed SPEDER converges faster and achieve the state-of-the-art performances in most of the environments, demonstrating the sample efficiency and the ability to balance of exploration vs. exploitation of SPEDER.

Table 4: Hyperparameters used for SPEDER in all the environments in MuJoCo and DM Control Suite.

	Hyperparameter Value
C	1.0
regularization coef	1.0
Bonus Coefficient (MuJoCo)	0.0
Bonus Coefficient (DM Control)	5.0
Actor lr	0.0003
Model lr	0.0003
Actor Network Size (MuJoCo)	(256, 256)
Actor Network Size (DM Control)	(1024, 1024)
SVD Embedding Network Size (MuJoCo)	(1024, 1024, 1024)
SVD Embedding Network Size (DM Control)	(1024, 1024, 1024)
Critic Network Size (MuJoCo)	(1024, 1)
Critic Network Size (DM Control)	(1024, 1)
Discount	0.99
Target Update Tau	0.005
Model Update Tau	0.005
Batch Size	256

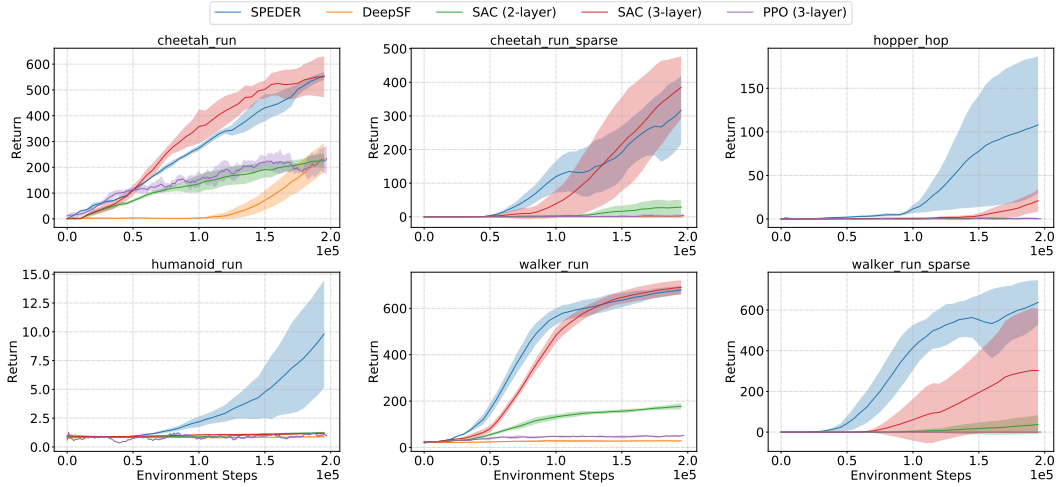


Figure 4: Performance Curves for online DM Control Suite.

E.3 Transition Estimation via Spectral Decomposition.

We show that the SPEDER objective can learn valid transitions of the environment. We use a empty-room maze environment, where the state is the position of the agent and the action is the velocity. The transition can be expressed as $s' = s + at + \epsilon$, where t is a fixed time interval and $\epsilon \sim \mathcal{N}(0, I)$. We run SPEDER for $100K$ steps and the learned transition heatmap is visualized in Figure 5.

From the figure, the high density region is centered around the red dot (target position S1), which means the representation learned by our objective captures the environment transition. This shows the spectral decomposition can learn a good transition function.

E.4 Imitation Learning

We provide the performance curves for imitation learning in Figures 6 and 7.

For TRAIL, OPAL, SPiRL, SKiLD, and BC, we used the same hyperparameters as reported in Yang et al. [2021]. For all methods, we pre-trained the representations for 200K steps using Adam optimizer with a learning rate of $3e-4$ and batch size 256. For latent behavioral cloning, we train the latent policy π_Z for 1M iterations using a learning rate of $1e-4$ for BC, SPiRL, SKiLD, and OPAL, and $3e-5$ for SPEDER and TRAIL (both EBM and Linear). We found that decaying the BC learning rate helped prevent overfitting for all methods. We evaluate the policy every 10K iterations by rolling out the policy in the environment for 10 episodes, and recording the average return. The representations

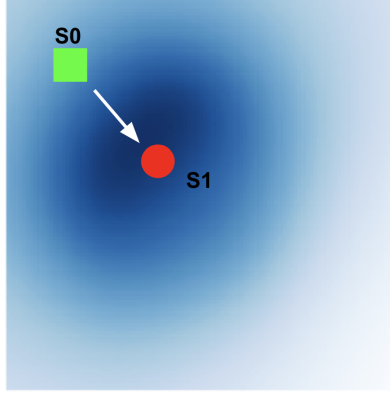


Figure 5: Estimated Transition via SPEDER. The blue region is the heatmap estimation via spectral decomposition and S1 is the target position of the agent.

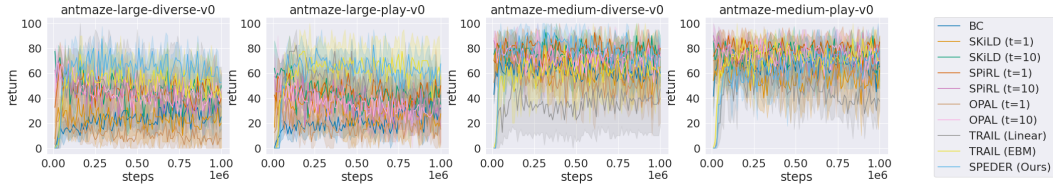


Figure 6: After pre-training, we train latent behavioral cloning on top of the learned representations for 1M iterations. BC refers to direct behavioral cloning on the expert dataset without latent representations. The corresponding barplot of the final performance is provided in Figure 1.

Table 5: Loss coefficients used for SPEDER (8). We denote the loss coefficients as a_1 for the $\mathbb{E}_{p(s')} [\mu(s')^\top \mu(s')] / (2d)$ term; a_2 for the $\mathbb{E}_{(s,a) \sim p_0} [\phi(s, a) \phi(s, a)^\top] = I_d / d$ term; and a_3 for the additional normalization regularization term in (9).

Domain	SPEDER w/o normalization		SPEDER w/ normalization (9)		
	a_1	a_2	a_1	a_2	a_3
antmaze-large-diverse	0.1	0.1	0.01	0.01	1.
antmaze-large-play	0.01	0.01	1.	0.01	1.
antmaze-medium-diverse	1.	0.01	0.1	1.	0.1
antmaze-medium-play	1.	0.01	1.	0.1	1.

ϕ and action decoder π_α were frozen during downstream behavioral cloning. All imitation learning results are reported over 4 seeds.

Both the action decoder π_α and the latent policy π_Z are parameterized as a multivariate Gaussian distribution, with the mean and variance approximated using a two-layer MLP network with hidden layer size 256.

For SPEDER and TRAIL, ϕ and μ are parameterized as a 2-layer MLP with hidden layer size 256, and a Swish activation function [Ramachandran et al., 2017] at the end of each hidden layer. We ran a sweep of embedding dimensions $d \in \{64, 256\}$ and found that $d = 64$ worked best for TRAIL, and $d = 256$ worked best for SPEDER. For SPEDER, we ran a sweep of coefficients for each loss term in (8), and summarize the coefficients used in Table 5. For TRAIL Linear, we used a Fourier dimension of 8192, which has been provided more preference, while still performing worse.

For SPiRL, SKiLD and OPAL, we used an embedding dimension of 8, which was reported to work best [Yang et al., 2021]. The trajectory encoder is parameterized as a bidirectional RNN, and the skill prior is parameterized as a Gaussian network following [Ajay et al., 2020]. SPiRL and SKiLD are adapted for downstream behavioral cloning by minimizing the KL divergence between the latent policy and the skill prior.

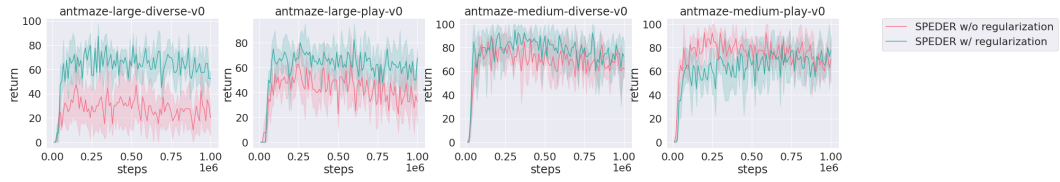


Figure 7: Performance curve of downstream behavioral cloning for SPEDER with vs. without normalized marginalization regularization (9). The corresponding barplot of the final performance is provided in Figure 2.